Parametric study of the wave dispersion in the hydro-elastic system consisting of an inhomogeneously prestressed hollow cylinder containing compressible inviscid fluid

Surkay D. Akbarov[*1,2] and Gurbaneli J. Veliyev[3a]

[1]*Department of Mechanical Engineering, Yildiz Technical University, 34349, Besiktas, Istanbul, Turkey*
[2]*Institute of Mathematics and Mechanics of the National Academy of Sciences of Azerbaijan,
AZ1141, Baku, Azerbaijan*
[3]*Baku State University, Baku, Azerbaijan*

Abstract. The present work is concerned with the study of the influence of inhomogeneous initial stresses in a hollow cylinder containing a compressible inviscid fluid on the propagation of axisymmetric longitudinal waves propagating in this cylinder. The study is carried out using the so-called three-dimensional linearized theory of elastic waves in bodies with initial stresses to describe the motion of the cylinder and using the linearized Euler equations to describe the flow of the compressible inviscid fluid. It is assumed that the inhomogeneous initial stresses in the cylinder are caused by the internal pressure of the fluid. To solve the corresponding eigenvalue problem, the discrete-analytic solution method is applied and the corresponding dispersion equation is obtained, which is solved numerically, after which the corresponding dispersion curves are constructed and analyzed. To obtain these dispersion curves, parameters characterizing the magnitude of the internal pressure, the ratio of the sound velocities in the cylinder material and in the fluid, and the ratio of the material densities of the fluid and the cylinder are introduced. Based on these parameters, the influence of the inhomogeneous initial stresses in the cylinder on the dispersion of the above-mentioned waves in the considered hydro-elastic system is investigated. Moreover, based on these results, appropriate conclusions about this influence are drawn. In particular, it is found that the character of the influence depends on the wavelength. Accordingly, the inhomogeneous initial stresses before (after) a certain value of the wavelength lead to a decrease (increase) of the wave propagation velocity in the zeroth and first modes.

Keywords: discrete-analytical method; hydro-elastic hollow cylinder-fluid system; inhomogeneous initial stresses; wave dispersion; compressible fluid

1. Introduction

To control oil, water and various types of chemical fluid production and transportation by pipelines requires the theoretical study of the corresponding dynamic problems of hydro-elastic systems consisting of the hollow cylinder and fluid. Similarly, such a study is required by the

---

∗Corresponding author, Professor, E-mail: akbarov@yildiz.edu.tr
[a]Ph.D., E-mail: vqurbaneli@gmail.com

corresponding biophysical problems related to the understanding of the flow of blood in a vein. Note that the studies on the dispersions of the waves propagating in the systems "hollow cylinder+fluid" have special importance among these studies. This is because the results of these studies form the theoretical basis for the non-destructive testing method for damage detection by acoustic and ultrasonic waves in pipelines transporting fluids.

We now briefly review related investigations, beginning this review with the paper (Lamb 1898) in which the dispersion of an axisymmetric wave propagating in a thin cylindrical shell containing a non-viscous compressible fluid was investigated. Note that in this work the motion of the shell was described in the framework of Kirchhoff-Love theory. In this description, the bending terms are omitted and the concrete results are presented for the low wavenumber cases. Note also that in this work the cases where the wave propagation velocity is smaller than the sound velocity in the fluid were considered, and approximate analytical expressions for the wave propagation velocity as a function of the wave number were obtained. In the context of the above assumptions, the paper (Lamb 1898) also considered the case where the cylindrical shell is immersed in a liquid. Moreover, in this work, the formulation of the problem for thick shells was developed in the framework of classical linear elastodynamics.

A significant development of the research carried out in the paper (Lamb 1898) was made in the paper (Lin and Morgan 1956). In this work, the corresponding problems were studied using the refined first-order shell theory. According to this theory, the shear deformation of the cross-section and its rotational inertia are taken into account in establishing the equation of motion of the shell. In this framework, concrete numerical results are obtained on the influence of shear deformation and rotational inertia on the corresponding dispersion curves.

Further development in this field focused on the use of more accurate models to describe the fluid flow and motion of a circular hollow cylinder and a review of the related investigations carried out until the last decade of the last century was made in the papers (Sinha *et al.* 1992) and (Plona *et al.* 1992). Note that in these papers, in addition to this review work, a theoretical study of the wave dispersion problems for the hydro-elastic system consisting of a hollow cylinder and a compressible inviscid fluid was carried out using the exact equations and relations of elastodynamics (Sinha *et al.* 1992). Experimental verification of the theoretical results (Plona *et al.* 1992) was also performed. In addition, we note that some of the recent studies conducted in the papers (Ahmet 2008, Selvamani 2016, Sandhyarani *et al.* 2019) and others listed therein have investigated similar problems for the cases where the cylinder material was more complex. However, all these studies were carried out using classical linear elastodynamics, in the framework of which the initial stresses in the cylinder cannot be taken into account when studying the dispersion of the waves propagating in this cylinder in contact with the fluid. Note that in cases where the cylinders contain or transport fluids at high pressure and a certain flow rate, as well as in very deep subsea pipelines, these cylinders (or pipelines) are subjected to hydrostatic pressures from the fluid side. These pressures cause static stress-strain states in the cylinders before the corresponding wave propagation begins. Therefore, these static stress-strain states are considered as the initial stress-strain state with respect to the additional dynamic perturbation state causing the wave propagation in the hydro-elastic system "cylinder+fluid", consideration of the influence of these initial stresses on the dispersion of waves cannot be done within the framework of the classical linear theory of elastodynamics, since this influence has a nonlinear character. For this purpose, the corresponding dynamic problems are modeled within the framework of geometrically nonlinear elastodynamics. Then, the corresponding field equations and relations are linearized with respect to the dynamic perturbations. As a result of this linearization, the so-called linearized

equations and relations are obtained for the study of the wave propagation problems in bodies with initial stresses. The initial stresses enter the coefficients of the obtained linearized equations and relations, and in this way, the influence of the initial stresses (or strains) on the dispersion of waves propagating in the bodies with initial stresses is considered. It should be noted that the above linearization procedures can be carried out both by means of approximate nonlinear shell theories and by means of the corresponding three-dimensional nonlinear exact equations of elastodynamics.

From the historical aspect, some of the earlier and valuable investigations carried out within the framework of the Kirchhoff-Love shell theory were made in the papers (Atabek and Lew 1966) and (Atabek 1968). Note that in the paper (Atabek and Lew 1966), the hydro-elastic system consisting of incompressible Newtonian viscous fluid and a tube made of isotropic and physically linear material was considered. Under this consideration it was assumed that the cylindrical shell has homogeneous circumferential and longitudinal initial normal stresses (without indicating the reasons causing these stresses) and an attempt was made to investigate how these initial stresses influence the velocity of the waves propagated in this hydro-elastic system. Numerical results are presented for the low-wavenumber approximation case for which the outgoing and the incoming waves appear. In particular, as a result of the analyses of the numerical results, it is established that in the cases where the initial stresses are stretching their existence causes the propagation velocity of the outgoing waves to decrease.

The paper (Atabek 1968) further developed the investigations carried out in the paper (Atabek and Lew 1966) for the case when the material of the cylindrical shell is an orthotropic one and the equation of motion of this shell is described in the framework of the uniformly distributed additional mass, a dashpot, and a spring model. Numerical results are also presented for the low wavenumber approximation and the influence of the anisotropy of the tube material on the wave propagation velocity is analyzed.

A similar problem for the case when the material of the tube is a highly elastic incompressible material was considered in the work (Rachev 1978) and the fluid contained in the cylinder was modeled as an incompressible viscous Newtonian. The studies are performed using the corresponding exact so-called 3D linearized equations and relations. More systematic studies on the dispersion of waves in a homogeneously prestressed highly elastic cylinder in contact with incompressible viscous Newtonian fluids were carried out in the papers (Bagno and Guz 1982), (Bagno *et al.* 1994) and in the papers listed in the reviews (Bagno and Guz 1997) and (Bagno and Guz 2016). Note that in these works the investigations are carried out also within the framework of the exact equations and relations of the three dimensional linearized theory of elastic waves in initially stressed bodies

With this, we limit ourselves here to the review of the studies related to the dynamics of the systems "hollow cylinder+fluid". At the same time, we note that the corresponding review of the studies on the dynamics of the systems "plate+fluid" can be found in the articles listed (Akbarov 2018, Akbarov and Huseynova 2019, 2020, Hazalic *et al.* 2018, Mandal and Maity 2015) and others listed therein.

In recent years, new investigations have also been carried out on the other aspects of the dynamics of the hollow cylinder containing a fluid. As an example of such research, the research carried out in the works (Darıcık *et al.* 2022, Bochkarev and Lekomtsev 2022, Gao *et al.* 2022) and others listed therein.

Wherein the paper (Darıcık *et al.* 2022) studies the stresses and deformations in a four-layer fiber-reinforced polymer composite pipe (hollow cylinder) caused by the pressurized sudden flow

of the fluid in this pipe. The aim of the paper's study (Gao 2022) is to simulate fluid flow in pipes with different boundary conditions. A free-pressure fluid model based on the Navier-Stokes equation is used in the paper. The corresponding mathematical problems are solved using the numerical method. A problem called "Stability of Pipes" is used to compare the frequency and critical fluid velocity.

The work (Bochkarev 2022) studies the dynamic behavior of laminated circular cylindrical composite shells interacting with a compressible inviscid fluid whose behavior is described by potential theory. The hydrodynamic pressure exerted by the fluid on the inner surface of the shell is calculated using the linearized Bernoulli equation. The semi-analytical finite element method is used to obtain numerical results about the natural vibration of the hydro-elastic system under consideration.

From the above overview of the dispersion of waves in the systems "pre-stressed hollow cylinder+fluid", it is clear that all these investigations were carried out within the framework of the assumption of homogeneity of the initial stresses in the cylinder. However, it is obvious that in many cases these stresses are inhomogeneous due to the internal or external fluid pressures, especially in the case of relatively thick cylinders. To the best of the authors' knowledge, there has been no study of wave propagation in an inhomogeneously pre-stressed hollow cylinder containing a fluid until the paper (Akbarov *et al.* 2021). Therefore, in the paper (Akbarov *et al.* 2021), an approach to studying the dynamic problems for hydro-elastic systems consisting of an inhomogeneously pre-stressed hollow cylinder containing a compressible inviscid fluid was proposed. This approach is based on the discrete-analytic solution method of the governing field equations for the cylinder. However, in the work (Akbarov *et al.*2021), only a few concrete numerical results on the dispersion of the axisymmetric longitudinal waves propagating in the mentioned hydro-elastic system were considered. In the present work, in order to obtain a comprehensive knowledge of the influence of the inhomogeneous initial stresses in the cylinder on the dispersion of the axisymmetric waves propagating in the system considered, parametric numerical investigations are carried out. These investigations are based on the approach developed in the paper (Akbarov *et al.* 2021) and the significance of the results presented is not limited to the specific materials selected. Under these investigations, the motion of the cylinder is described by the three-dimensional linearized theory of elastic waves in initially stressed bodies, and the flow of the fluid is described by the linearized Euler equations for the compressible inviscid fluid. The corresponding dispersion equation is obtained and this equation is solved numerically as a result of which the corresponding dispersion curves are constructed and analyzed. To obtain these dispersion curves, parameters are introduced that characterize the magnitude of the internal hydrostatic pressure, the ratio of the sound velocities in the cylinder material and in the fluid, and the ratio of the fluid and cylinder densities. Namely, these parameters are used to illustrate the influence of the inhomogeneous initial stresses in the cylinder on the dispersion of the above-mentioned waves in the considered hydro-elastic system.

2. Mathematical formulation of the problem

Consider the hydro-elastic system consisting of an infinite hollow cylinder filled with the compressible barotropic inviscid fluid. Associate the cylindrical $Or\theta z$ and Cartesian $Ox_1x_2x_3$ ($x_3 = z$) (Fig. 1) system of coordinates with the central axis of the cylinder. We use the Lagrange coordinates for indicating the location of the points of the cylinder and the Euler coordinates for
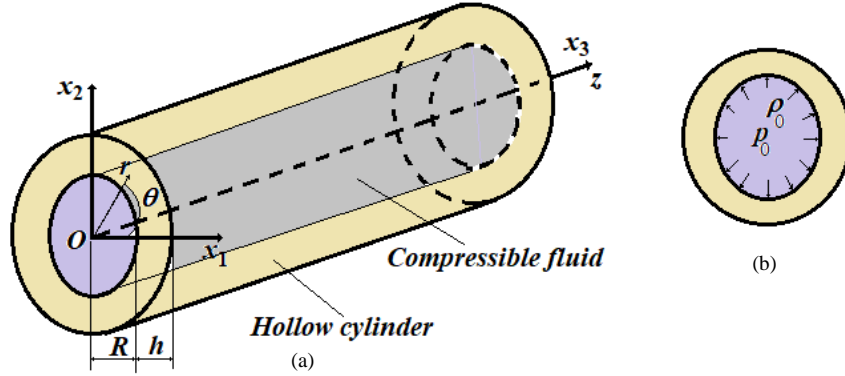
Fig. 1 The sketch of the hydro-elastic system under consideration

indicating the location of the fluid particles. We distinguish two states of the hydro-elastic system, in the first of which it is assumed that the fluid is at rest and acts on the interior of the cylinder with pressure p_0 and the density of this fluid is ρ_0, and this state is named as the initial state. We assume that the pressure of the fluid causes the initial axisymmetric static stress state in the cylinder. Below we will use the upper index "0" for indicating the quantities regarding this initial state in the cylinder and the stresses in this state, according to (Timoshenko and Goodier 1951), can be determined through the following expressions which are obtained from the solution of the corresponding Lame problem in the classical linear theory of elasticity.

$$\sigma_{rr}^0 = \frac{p_0}{(1+h/R)^2-1}\left(1-\frac{R^2}{r^2}\left(1+\frac{h}{R}\right)^2\right), \sigma_{\theta\theta}^0 = \frac{p_0}{(1+h/R)^2-1}\left(1+\frac{R^2}{r^2}\left(1+\frac{h}{R}\right)^2\right),$$
$$\sigma_{zz}^0 = \nu(\sigma_{rr}^0 + \sigma_{\theta\theta}^0). \tag{1}$$

Note that the conventional notation is used in (1) and some parameters which enter into these expressions are indicated in Fig. 1.

We assume that after the foregoing initial state appears, the system gets a certain dynamical perturbation as a result of which the axisymmetric longitudinal waves propagate therein (the second state). The problem consists of how the initial stresses determined by the expressions in (1) influence the propagation of these waves, i.e., the dispersion of these waves. As mentioned before, to determine this influence we try to use the exact linearized 3D equations and relations of the theory of elastic waves in bodies with initial stresses and the linearized equations of motion of barotropic inviscid fluids.

Thus, according to the monographs (Eringen and Suhubi 1975, Guz 2004, Akbarov 2015), and others listed therein, we write the 3D linearized field equations and relations of the elastic wave propagation which are satisfied in the region occupied by the cylinder.

The equations of motion

$$\frac{\partial t_{rr}}{\partial r} + \frac{\partial t_{zr}}{\partial z} + \frac{1}{r}(t_{rr} - t_{\theta\theta}) = \rho\frac{\partial^2 u_r}{\partial t^2}, \frac{\partial t_{rz}}{\partial r} + \frac{1}{r}t_{rz} + \frac{\partial t_{zz}}{\partial z} = \rho\frac{\partial^2 u_z}{\partial t^2}, \tag{2}$$

where

$$t_{rr} = \sigma_{rr} + \sigma_{rr}^0(r)\frac{\partial u_r}{\partial r}, t_{rz} = \sigma_{rz} + \sigma_{rr}^0(r)\frac{\partial u_z}{\partial r}, t_{\theta\theta} = \sigma_{\theta\theta} + \sigma_{\theta\theta}^0(r)\frac{u_r}{r},$$

$$t_{zr} = \sigma_{zr} + \sigma_{zz}^0(r)\frac{\partial u_r}{\partial z}, t_{zz} = \sigma_{zz} + \sigma_{zz}^0(r)\frac{\partial u_z}{\partial z}. \tag{3}$$

The elasticity relations

$$\sigma_{(jj)} = \lambda(\varepsilon_{rr} + \varepsilon_{\theta\theta} + \varepsilon_{zz}) + 2\mu\varepsilon_{(jj)}, (jj) = rr; \theta\theta; zz, \sigma_{rz} = 2\mu\varepsilon_{rz} \tag{4}$$

The strain-displacement relations

$$\varepsilon_{rr} = \frac{\partial u_r}{\partial r}, \varepsilon_{\theta\theta} = \frac{u_r}{r}, \varepsilon_{zz} = \frac{\partial u_z}{\partial z}, \varepsilon_{rz} = \frac{1}{2}\left(\frac{\partial u_r}{\partial z} + \frac{\partial u_z}{\partial r}\right). \tag{5}$$

The Eqs. (2)-(5) compose the complete system of the linearized field equations for describing the motion of the cylinder. Note that in (2) and (3) the notation $t_{rr}, t_{rz}, t_{\theta\theta}, t_{zr}$ and t_{zz} shows the components of the non-symmetric Kirchhoff stress tensor. The other notation used in (2)-(5) is conventional.

Now, according to (Guz 2009), consider the linearized field equations for the barotropic compressible inviscid fluid flow.

The continuity equation

$$\frac{\partial \rho'}{\partial t} + \rho_0\left(\frac{\partial V_r}{\partial r} + \frac{V_r}{r} + \frac{\partial V_z}{\partial z}\right) = 0 \; ; \tag{6}$$

Linearized equations of the fluid flow

$$\frac{\partial V_r}{\partial t} = -\frac{1}{\rho_0}\frac{\partial p'}{\partial r}, \frac{\partial V_z}{\partial t} = -\frac{1}{\rho_0}\frac{\partial p'}{\partial z}. \tag{7}$$

The state equation

$$a_0^2 = \frac{\partial p'}{\partial \rho'}, \tag{8}$$

where a_0 is the sound speed in the fluid, ρ' and p' are the perturbations of the fluid density and the fluid pressure, respectively, and V_r, and V_z are the components of the velocity vector.

In this way, we obtain the complete system of Eqs. (6)-(8) through which the flow of the fluid is described. Now we attempt to formulate the corresponding boundary and compatibility conditions. In connection with this, we can write the following boundary conditions on the external surface of the cylinder.

$$t_{rr}|_{r=R+h} = 0, t_{rz}|_{r=R+h} = 0. \tag{9}$$

Using the notation indicated in Fig. 1, we can write the following compatibility conditions.

$$t_{rr}|_{r=R} = -p', t_{rz}|_{r=R} = 0, \frac{\partial u_r}{\partial t}\bigg|_{r=R} = V_r|_{r=R}. \tag{10}$$

Moreover, the following conditions on the boundedness of the quantities related to the fluid at the central axis of the cylinder must be satisfied.

$$\{|p'|, |\rho'|, |V_r|, |V_z|\}|_{r=0} < \infty . \tag{11}$$

The first and second conditions in (10) imply continuity of the force vector at the fluid-cylinder interface. According to this continuity condition, the perturbation of the radial normal stress t_{rr} in the cylinder is set equal to the perturbation of the radial normal stress of the fluid, which is equal to $-p'$ at the interface (the first condition). Since the fluid is assumed to be non-viscous, the shear stress in the fluid is zero and, according to the continuity of the force vector, the shear stress in the cylinder at the interface is also set equal to zero (the second condition in (10)). The third condition

in (10) means the equality of the normal velocities of the components of the hydro-elastic system at the interface. This condition can also be considered as a generalization of the well-known impermeability condition for inviscid fluids. However, for inviscid fluids, such a condition does not satisfy the velocities in the tangent direction to the interface, i.e., in the case considered here for the velocities in the direction of the Oz axis. In other words, for the inviscid fluids, the fluid velocity V_z is not equal to the $\frac{\partial u_z}{\partial t}$ at the fluid-cylinder interface.

Recall that we consider the problem of axisymmetric wave propagation, where all the sought quantities of the problem do not depend on the coordinate θ, and the stress $t_{r\theta}$, the displacement u_θ, and the velocity V_θ are set equal to zero. Therefore, the stress $t_{r\theta}$, the displacement u_θ, and the velocity V_θ are not involved in the conditions in (9), (10), and (11).

Note that in the problem under consideration the sought values depend only on two spatial coordinates r and z. Nevertheless, it is noted above that the "three-dimensional linearized theory of elastic waves in bodies with initial stresses" is used to study the problem. This is because in all the corresponding references (see, for example, (Guz 2004, Akbarov 2015) and many other references listed there) this term is used as it is above, although the problem is two-dimensional in spatial coordinates. In these references and in the present paper, the use of the above term means that the equations of motion for the pre-stressed cylinder are not obtained by linearizing the nonlinear equations and relations of the various approximate shell theories, but from the nonlinear equations and relations of the exact equations and relations of elastodynamics.

This completes the mathematical formulation of the problem under consideration.

3. The solution method of the formulated problem

In general, the solution to the dynamic problems of the hydro-elastic system requires the involvement of various types of numerical and approximate-analytical solution methods, a review of which can be found in the paper (Kumar and Sriram 2020). In this sense, in the present paper, we prefer to use the approximate-analytical method, i.e., the so-called discrete-analytical method proposed and employed in the papers (Akbarov and Bagirov 2019, Akbarov *et al.* 2021) for the solution to the system of Eqs. (2)-(5). The essence of this method is to reduce the solution of the system of equations with variable coefficients to the solution of a certain number of corresponding equations with constant coefficients. Now, step by step, we will consider the application of this method.

3.1 Dividing the region occupied by the cylinder into sub-regions

Based on the paper (Akbarov and Bagirov 2019, Akbarov *et al.* 2021), we divide the region $[R, R + h]$ into N number of sub-regions (or sub-layers) with h/N thickness and within the framework of the $n - th$ sub-layer the relation $(R + (n - 1)h/N \leq r \leq (R + nh/N)$ takes place, where $1 \leq n \leq N$. Taking the insignificance of the initial stress changes within each sublayer into consideration, we assume that these stresses can be taken approximately as constants within these sub-layers, the values of which are determined by the following relations

$$\sigma_{rr}^0(r) \approx \sigma_{rr}^0(r_n), \sigma_{\theta\theta}^0(r) \approx \sigma_{\theta\theta}^0(r_n), \sigma_{zz}^0(r) \approx \sigma_{zz}^0(r_n),$$
$$r_n = R + (n - 1)h/N + h/(2N). \tag{12}$$

After the foregoing division procedure, we formulate the contact and boundary conditions which are satisfied between the sub-layers and on the face of the sub-layers.

Taking the relations in (10) and (11) into consideration, the contact conditions on the sub-layers' interface, the boundary conditions on the outer face of the outer sub-layer and the compatibility conditions on the inner face of the inner sub-layer can be written as follows.

$$t_{rr}^1|_{r=R} = -p', \; t_{rz}^1|_{r=R} = 0, \; \frac{\partial u_r^1}{\partial t}\bigg|_{r=R} = V_r|_{r=R}, \; t_{rr}^1|_{r=R+h/N} = t_{rr}^2|_{r=R+h/N},$$

$$t_{rz}^1|_{r=R+h/N} = t_{rz}^2|_{r=R+h/N}, \; u_r^1|_{r=R+h/N} = u_r^2|_{r=R+h/N},$$

$$u_z^1|_{r=R+h/N} = u_z^2|_{r=R+h/N}, \cdots,$$

$$t_{rr}^{n-1}|_{r=R+(n-1)h/N} = t_{rr}^n|_{r=R+(n-1)h/N}, \; t_{rz}^{n-1}|_{r=R+(n-1)h/N} = t_{rz}^n|_{r=R+(n-1)h/N},$$

$$u_r^{n-1}|_{r=R+(n-1)h/N} = u_r^n|_{r=R+(n-1)h/N}, \; u_z^{n-1}|_{r=R+(n-1)h/N} = u_z^n|_{r=R+(n-1)h/N}, \cdots,$$

$$t_{rr}^N|_{r=R+h} = 0, \; t_{rz}^N|_{r=R+h} = 0. \tag{13}$$

The upper indices in $1, 2, \ldots, N$ in (13) indicate the number of sublayers. The number of relations in (13) is equal to $4N + 1$ where the value of N is defined from the convergence requirement of the numerical results and the upper indices in these relations indicate the number of the corresponding sub-layer.

Thus, within the assumptions (12) and (13), we consider the solution to the system of equations (2)-(5).

3.2 Solution procedure to the system of Eqs. (2)-(5) within each sublayer

First of all, we note that the assumption (12) allows us to reduce the system of Eqs. (2)-(5) with variable coefficients to the corresponding system of equations with constant coefficients within the framework of each sub-layer. Consequently, taking the assumption (12) into account, we obtain the following system of equations with constant coefficients from the Eqs. (2) and (3), which are satisfied within the framework of each sublayer separately.

$$\frac{\partial \sigma_{rr}^n}{\partial r} + \sigma_{rr}^0(r_n)\frac{\partial^2 u_r^n}{\partial r^2} + \frac{\partial \sigma_{zr}^n}{\partial z} + \sigma_{zz}^0(r_n)\frac{\partial^2 u_r^n}{\partial z^2} + \frac{1}{r}(\sigma_{rr}^n - \sigma_{\theta\theta}^n) +$$

$$\sigma_{rr}^0(r_n)\frac{1}{r}\frac{\partial u_r^n}{\partial r} - \sigma_{\theta\theta}^0(r_n)\frac{u_r^n}{r^2} = \rho\frac{\partial^2 u_r^n}{\partial t^2},$$

$$\frac{\partial \sigma_{rz}^n}{\partial r} + \sigma_{rr}^0(r_n)\frac{\partial^2 u_z^n}{\partial r^2} + \frac{1}{r}\sigma_{rz}^n + \sigma_{rr}^0(r_n)\frac{1}{r}\frac{\partial u_z^n}{\partial r} + \frac{\partial \sigma_{zz}^n}{\partial z} +$$

$$\sigma_{zz}^0(r_n)\frac{\partial^2 u_z^n}{\partial z^2} = \rho\frac{\partial^2 u_z^n}{\partial t^2}. \tag{14}$$

Rewriting the relations (4) and (5) with the corresponding upper indices within the framework of each sub-layer separately and connecting those with (14) we obtain the complete system of equations for determination of the sought quantities within the scope of each layer.

Now we attempt to solve these systems of equations and for this purpose we use the well-known classical Lame decomposition which can be found in each monograph related to elastodynamics (see, for instance the monograph (Eringen and Suhubi 1975)). Note that this decomposition for the axisymmetric problems can be written as follows.

$$u_r^n = \frac{\partial \Phi^n}{\partial r} + \frac{\partial^2 \Psi^n}{\partial r \partial z}, \; u_z^n = \frac{\partial \Phi^n}{\partial z} - \frac{\partial^2 \Psi^n}{\partial r^2} - \frac{\partial \Psi^n}{r \partial r}. \tag{15}$$

Thus, using the expressions (15), (4) and (3) and doing some cumbersome mathematical

manipulations, we obtain the following equations for determination of the potentials Φ^n and Ψ^n

$$
\left(1+\frac{\sigma_{rr}^0(r_n)}{\lambda+2\mu}\right)\frac{\partial^2\Phi^n}{\partial r^2}+\left(1+\frac{\sigma_{\theta\theta}^0(r_n)}{\lambda+2\mu}\right)\frac{\partial\Phi^n}{r\partial r}+\left(1+\frac{\sigma_{zz}^0(r_n)}{\lambda+2\mu}\right)\frac{\partial^2\Phi^{n_i}}{\partial z^2}=\frac{1}{(c_1)^2}\frac{\partial^2\Phi^n}{\partial t^2},
$$

$$
\left(1+\frac{\sigma_{rr}^0(r_n)}{\mu}\right)\frac{\partial^2\Psi^n}{\partial r^2}+\left(1+\frac{\sigma_{\theta\theta}^0(r_n)}{\mu}\right)\frac{\partial\Psi^n}{r\partial r}+\left(1+\frac{\sigma_{zz}^0(r_n)}{\mu}\right)\frac{\partial^2\Psi^n}{\partial z^2}=\frac{1}{(c_2)^2}\frac{\partial^2\Psi^n}{\partial t^2}, \qquad (16)
$$

where $c_1=\sqrt{(\lambda+2\mu)/\rho}$ and $c_2=\sqrt{\mu/\rho}$ are the speeds of the dilatation and distortion wave propagation velocities, respectively, of the cylinder's material.

If we assume that $\sigma_{zz}^0(r_n)=0$, $\sigma_{rr}^0(r_n)=0$ and $\sigma_{\theta\theta}^0(r_n)=0$, then the equations in (16) coincide with the corresponding equations in classical elastodynamics (see, for instance (Eringen and Suhubi 1975)).

Representing the functions $\Phi^n, u_r^n, u_\theta^n, \sigma_{rr}^n, \sigma_{\theta\theta}^n$ and σ_{zz}^n with the multiplying $\sin(kz-\omega t)$ and the functions ψ^n, u_z^n and σ_{rz}^n with the multiplying $\cos(kz-\omega t)$, and denoting the amplitudes of these quantities with the same symbols, the following equations for the amplitudes of the potentials Φ^n and Ψ^n are obtained.

$$
\left(1+\frac{\sigma_{rr}^0(r_n)}{\lambda+2\mu}\right)\frac{d^2\Phi^n}{d(kr)^2}+\left(1+\frac{\sigma_{\theta\theta}^0(r_n)}{\lambda+2\mu}\right)\frac{d\Phi^n}{krd(kr)}+\left(\frac{1}{(c_1)^2}\frac{\omega^2}{k^2}-1-\frac{\sigma_{zz}^0(r_n)}{\lambda+2\mu}\right)\Phi^n=0,
$$

$$
\left(1+\frac{\sigma_{rr}^0(r_n)}{\mu}\right)\frac{d^2\Psi^n}{d(kr)^2}+\left(1+\frac{\sigma_{\theta\theta}^0(r_n)}{\mu}\right)\frac{d\Psi^n}{krd(kr)}+\left(\frac{1}{(c_2)^2}\frac{\omega^2}{k^2}-1-\frac{\sigma_{zz}^0(r_n)}{\mu}\right)\Psi^n=0. \qquad (17)
$$

Introducing the notation

$$
\alpha(r_n)=\frac{1+\sigma_{\theta\theta}^0(r_n)/\mu}{1+\sigma_{rr}^0(r_n)/\mu}, \beta(r_n)=\frac{1+\sigma_{zz}^0(r_n)/\mu}{1+\sigma_{rr}^0(r_n)/\mu}, r_1^n=kr\sqrt{\frac{c^2}{(c_2)^2(1+\sigma_{rr}^0(r_n)/\mu)}-(\beta(r_n))^2}\ , c=\omega/\kappa,
$$

$$
\alpha_1(r_n)=\frac{1+\sigma_{\theta\theta}^0(r_n)/(\lambda+2\mu)}{1+\sigma_{rr}^0(r_n)/(\lambda+2\mu)}, \beta_1(r_n)=\frac{1+\sigma_{zz}^0(r_n)/(\lambda+2\mu)}{1+\sigma_{rr}^0(r_n)/(\lambda+2\mu)}
$$

$$
r_2^n=kr\sqrt{\frac{c^2}{(c_1)^2(1+\sigma_{rr}^0(r_n)/(\lambda+2\mu))}-(\beta_1(r_n))^2}, \qquad (18)
$$

we simplify the expressions of the equations in (17) as follows.

$$
\frac{d^2\Phi^n}{d(r_2)^2}+\frac{\alpha_1(r_n)}{r_2}\frac{d\Phi^n}{dr_2}+\Phi^n=0, \quad \frac{d^2\Psi^n}{d(r_1)^2}+\frac{\alpha(r_n)}{r_1}\frac{d\Psi^n}{dr_1}+\Psi^n=0. \qquad (19)
$$

According to (Watson 1966), we use the representation

$$
\Phi^n(r_2)=(r_2)^{(1-\alpha_1(r_n))/2}\Phi_1^n(r_2), \Psi^n(r_1)=(r_1)^{(1-\alpha(r_n))/2}\Psi_1^n(r_1) \qquad (20)
$$

and substituting them into the Eq. (19), the following Bessel equations are obtained for the unknown functions $\Phi_1^n(r_2)$ and $\Psi_1^n(r_1)$.

$$
\frac{d^2\Phi_1^{(i)n_i}}{d(r_2^{(i)})^2}+\frac{1}{r_2^{(i)}}\frac{d\Phi_1^{(i)n_i}}{dr_2^{(i)}}+\left(1-\frac{(1-(\alpha_1^{(i)}(r_{n_i}))^2/4}{(r_2^{(i)})^2}\right)\Phi_1^{(i)n_i}=0,
$$

$$
\frac{d^2\Psi_1^{(i)n_i}}{d(r_1^{(i)})^2}+\frac{1}{r_1^{(i)}}\frac{d\Psi_1^{(i)n_i}}{dr_1^{(i)}}+\left(1-\frac{(1-(\alpha^{(i)}(r_{n_i}))^2/4}{(r_1^{(i)})^2}\right)\Psi_1^{(i)n_i}=0. \qquad (21)
$$

Thus, using the solutions to the equations in (21) determined through the Bessel functions and substituting them into the presentations in (20) we find the following expressions for the potentials Φ^n and Ψ^n.

$$\Phi^n = A_1^n (r_2)^{\gamma_1(r_n)} E_{\gamma_1(r_n)}(r_2^{n_i}) + A_2^n (r_2)^{\gamma_1(r_n)} F_{\gamma_1(r_n)}(r_2^n),$$
$$\Psi^n = B_1^n (r_1)^{\gamma(r_n)} E_{\gamma(r_n)}(r_1^n) + B_2^n (r_1)^{\gamma(r_n)} F_{\gamma(r_n)}(r_1^n), \tag{22}$$

where

$$\gamma_1(r_n) = (1 - \alpha_1(r_n))/2, \gamma(r_n) = (1 - \alpha(r_n))/2$$

$$E_{\gamma_1(r_n)}(r_2^n) = \begin{cases} J_{\gamma_1(r_n)}(r_2^n) if (r_2^n)^2/r^2 > 0 \\ I_{\gamma_1(r_n)}(r_2^n) if (r_2^n)^2/r^2 < 0 \end{cases},$$

$$F_{\gamma_1(r_n)}(r_2^n) = \begin{cases} Y_{\gamma_1(r_n)}(r_2^n) if (r_2^n)^2/r^2 > 0 \\ K_{\gamma_1(r_n)}(r_2^n) if (r_2^n)^2/r^2 < 0 \end{cases},$$

$$E_{\gamma(r_n)}(r_1^n) = \begin{cases} J_{\gamma(r_n)}(r_1^n) if (r_1^n)^2/r^2 > 0 \\ I_{\gamma(r_n)}(r_1^n) if (r_1^n)^2/r^2 < 0 \end{cases},$$

$$F_{\gamma(r_n)}(r_1^{n_i}) = \begin{cases} Y_{\gamma(r_{n_i})}(r_1^n) if (r_1^n)^2/r^2 > 0 \\ K_{\gamma(r_n)}(r_1^n) if (r_1^{n_i})^2/r^2 < 0 \end{cases}. \tag{23}$$

In (23), $J_\delta(x)$ and $I_\delta(x)$ are the Bessel and modified Bessel functions of the first kind, however, $Y_\delta(x)$ and $K_\delta(x)$ are also Bessel and modified Bessel functions of the second kind.

3.3 The expressions for the displacements and stresses

Thus, substituting the expressions in (22) and (23) into (15) and using the relations (4) and (5) we determine the following expressions for the displacements and stresses existing within each separate sublayer through which are expressed the contact, boundary and compatibility conditions satisfied between the sublayers.

$$u_r^n(r) =$$

$$A_1^n \frac{dr_2^n}{dr} \left[\gamma_1(r_n)(r_2^n)^{(\gamma_1(r_n)-1)} E_{\gamma_1(r_n)}(r_2^n) + (r_2^{(n)})^{\gamma_1(r_n)} \frac{dE_{\gamma_1(r_n)}(r_2^n)}{dr_2^n} \right] +$$

$$A_2^n \frac{dr_2^n}{dr} \left[\gamma_1(r_n)(r_2^n)^{(\gamma_1(r_n)-1)} F_{\gamma_1(r_n)}(r_2^n) + (r_2^n)^{\gamma_1(r_n)} \frac{dF_{\gamma_1(r_n)}(r_2^n)}{dr_2^n} \right] +$$

$$B_1^n \frac{dr_1^n}{dr} \left[\gamma(r_n)(r_1^n)^{(\gamma(r_n)-1)} E_{\gamma(r_n)}(r_1^n) + \right.$$

$$(r_1^n)^{\gamma_1(r_n)} \frac{dF_{\gamma(r_n)}(r_1^n)}{dr_1^n} \left] + B_2^n \frac{dr_1^n}{dr} \left[\gamma(r_n)(r_1^n)^{(\gamma(r_n)-1)} F_{\gamma(r_n)}(r_1^n) + (r_1^n)^{\gamma(r_n)} \frac{dF_{\gamma(r_n)}(r_1^n)}{d(r_1^n)} \right],$$

$$u_z^n(r) = A_1^n (r_2^n)^{\gamma_1(r_n)} E_{\gamma_1(r_n)}(r_2^n) + A_2^n (r_2^n)^{\gamma_1(r_n)} F_{\gamma_1(r_n)}(r_2^n) -$$

$$B_1^n \left[\gamma(r_n)(\gamma(r_n) - 1) \left(\frac{dr_2^n}{dr} \right)^2 E_{\gamma(r_n)}(r_1^n) + \gamma(r_{n_i})(r_1^n)^{(\gamma(r_n)-1)} \times \right.$$

$$\frac{1}{r} E_{\gamma(r_n)}(r_1^n) + 2\gamma(r_n) \left(\frac{dr_1^n}{dr} \right)^2 \frac{dE_{\gamma(r_n)}(r_1^n)}{d(r_1^n)} + \frac{1}{r}(r_1^n)^{\gamma(r_n)} \times$$

$$\frac{dr_1^n}{dr} \frac{dE_{\gamma(r_n)}(r_1^n)}{d(r_1^n)} + (r_1^n)^{\gamma(r_n)} \left(\frac{dr_1^n}{dr} \right)^2 \frac{d^2 E_{\gamma(r_n)}(r_1^n)}{d(r_1^n)^2} \right] -$$

$$B_2^n \left[\gamma(r_n)(\gamma(r_n) - 1) \left(\frac{dr_2^n}{dr} \right)^2 F_{\gamma(r_n)}(r_1^n) + \gamma(r_n)(r_1^n)^{(\gamma(r_n)-1)} \times \right.$$

$$\frac{1}{r} F_{\gamma(r_n)}(r_1^n) + 2\gamma(r_n) \left(\frac{dr_1^n}{dr} \right)^2 \frac{dF_{\gamma(r_n)}(r_1^n)}{d(r_1^n)} + \frac{1}{r}(r_1^n)^{\gamma(r_n)} \times$$

$$\frac{dr_1^n}{dr} \frac{dF_{\gamma(r_n)}(r_1^n)}{d(r_1^n)} + (r_1^n)^{\gamma(r_n)} \left(\frac{dr_1^n}{dr} \right)^2 \frac{d^2 F_{\gamma(r_n)}(r_1^n)}{d(r_1^n)^2} \right],$$

$$\frac{\sigma_{rr}^n(r)}{\mu} = A_1^n \left\{ \left(\frac{dr_2^n}{dr}\right)^2 2\left(1+\frac{\lambda}{2\mu}\right) \left[\gamma_1(r_n)(\gamma_1(r_n)-1)(r_2^n)^{(\gamma_1(r_n)-2)} E_{\gamma_1(r_n)}(r_2^n) + \right. \right.$$

$$\left. 2\gamma_1(r_n)(r_2^n)^{(\gamma_1(r_n)-1)} \frac{dE_{\gamma_1(r_n)}(r_2^n)}{d(r_2^n)} + (r_2^n)^{\gamma_1(r_n)} \frac{d^2 E_{\gamma_1(r_n)}(r_2^n)}{d(r_2^n)^2}\right] + $$

$$\frac{\lambda}{\mu}\frac{1}{r_2^n}\left(\frac{dr_2^n}{dr}\right)^2 \left[\gamma_1(r_n)(r_2^n)^{(\gamma_1(r_n)-1)} E_{\gamma_1(r_n)}(r_2^n) + r_2^n \frac{dE_{\gamma_1(r_n)}(r_2^n)}{d(r_2^n)}\right] + \frac{\lambda}{\mu}(r_2^n)^{\gamma_1(r_n)} E_{\gamma_1(r_n)}(r_2^n)\right\} + $$

$$A_2^n \left\{ \left(\frac{dr_2^n}{dr}\right)^2 2\left(1+\frac{\lambda}{2\mu}\right) \left[\gamma_1(r_n)(\gamma_1(r_n)-1)(r_2^n)^{(\gamma_1(r_n)-2)} F_{\gamma_1(r_n)}(r_2^n) + \right.\right.$$

$$\left. 2\gamma_1(r_n)(r_2^n)^{(\gamma_1(r_n)-1)} \frac{dF_{\gamma_1(r_n)}(r_2^n)}{d(r_2^n)} + (r_2^n)^{\gamma_1(r_n)} \frac{d^2 F_{\gamma_1(r_n)}(r_2^n)}{d(r_2^n)^2}\right] + $$

$$\frac{\lambda}{\mu}\frac{1}{r_2^n}\left(\frac{dr_2^{n_i}}{dr}\right)^2 \left[\gamma_1(r_n)(r_2^n)^{(\gamma_1(r_n)-1)} F_{\gamma_1(r_n)}(r_2^n) + r_2^n \frac{dF_{\gamma_1(r_n)}(r_2^n)}{d(r_2^n)}\right] + \frac{\lambda}{\mu}(r_2^n)^{\gamma_1(r_n)} F_{\gamma_1(r_n)}(r_2^n)\right\} + $$

$$B_1^n \left\{ \left(\frac{dr_1^n}{dr}\right)^2 2\left(1+\frac{\lambda}{2\mu}\right) \left[\gamma(r_n)(\gamma(r_n)-1)(r_1^n)^{(\gamma(r_n)-2)} E_{\gamma(r_n)}(r_1^n) + \right.\right.$$

$$\left. 2\gamma(r_n)(r_1^n)^{(\gamma(r_n)-1)} \frac{dE_{\gamma(r_n)}(r_1^n)}{d(r_1^n)} + (r_1^n)^{\gamma(r_n)} \frac{d^2 E_{\gamma(r_n)}(r_1^n)}{d(r_1^n)^2}\right] + $$

$$\frac{\lambda}{\mu}\frac{1}{r_1^n}\left(\frac{dr_1^n}{dr}\right)^2 \left[\gamma(r_n)(r_1^n)^{(\gamma(r_n)-1)} E_{\gamma(r_n)}(r_1^n) + r_1^n \frac{dE_{\gamma(r_n)}(r_1^n)}{d(r_1^n)}\right] + $$

$$\frac{\lambda}{\mu}\left[\gamma(r_n)(\gamma(r_n)-1)(r_1^n)^{(\gamma(r_n)-2)} E_{\gamma(r_n)}(r_1^n) + \right.$$

$$\gamma(r_n)(r_1^n)^{(\gamma(r_n)-1)} \frac{1}{r_1^n}\left(\frac{dr_1^n}{dr}\right)^2 E_{\gamma(r_n)}(r_1^n) + 2\gamma(r_n)(r_1^n)^{(\gamma(r_n)-1)} \times $$

$$\left(\frac{dr_1^n}{dr}\right)^2 \frac{dE_{\gamma(r_n)}(r_1^n)}{d(r_1^n)} + \frac{1}{r_1^n}\left(\frac{dr_1^n}{dr}\right)^2 (r_1^n)^{\gamma(r_n)} \frac{dE_{\gamma(r_n)}(r_1^n)}{d(r_1^n)} + \left(\frac{dr_1^n}{dr}\right)^2 (r_1^n)^{\gamma(r_n)} \frac{d^2 E_{\gamma(r_n)}(r_1^n)}{d(r_1^n)^2}\right]\right\} + $$

$$B_2^n \left\{ \left(\frac{dr_1^n}{dr}\right)^2 2\left(1+\frac{\lambda}{2\mu}\right) \left[\gamma(r_n)(\gamma(r_n)-1)(r_1^n)^{(\gamma(r_n)-2)} F_{\gamma(r_n)}(r_1^n) + \right.\right.$$

$$\left. 2\gamma(r_n)(r_1^n)^{(\gamma(r_n)-1)} \frac{dF_{\gamma(r_n)}(r_1^n)}{d(r_1^n)} + (r_1^n)^{\gamma(r_n)} \frac{d^2 F_{\gamma(r_n)}(r_1^n)}{d(r_1^n)^2}\right] + $$

$$\frac{\lambda}{\mu}\frac{1}{r_1^n}\left(\frac{dr_1^n}{dr}\right)^2 \left[\gamma(r_n)(r_1^n)^{(\gamma(r_n)-1)} F_{\gamma(r_n)}(r_1^n) + r_1^n \frac{dF_{\gamma(r_n)}(r_1^n)}{d(r_1^n)}\right] + $$

$$\frac{\lambda}{\mu}\left[\gamma(r_n)(\gamma(r_n)-1)(r_1^n)^{(\gamma(r_n)-2)} F_{\gamma(r_n)}(r_1^n) + \right.$$

$$\gamma(r_n)(r_1^{n})^{(\gamma(r_n)-1)} \frac{1}{r_1^n}\left(\frac{dr_1^n}{dr}\right)^2 F_{\gamma(r_n)}(r_1^n) + 2\gamma(r_n)(r_1^n)^{(\gamma(r_n)-1)} \times $$

$$\left(\frac{dr_1^n}{dr}\right)^2 \frac{dF_{\gamma(r_n)}(r_1^n)}{d(r_1^n)} + \frac{1}{r_1^n}\left(\frac{dr_1^n}{dr}\right)^2 (r_1^n)^{\gamma(r_n)} \frac{dF_{\gamma(r_n)}(r_1^n)}{d(r_1^n)} + \left(\frac{dr_1^n}{dr}\right)^2 (r_1^n)^{\gamma(r_n)} \frac{d^2 F_{\gamma(r_n)}(r_1^n)}{d(r_1^n)^2}\right]\right\},$$

$$\frac{\sigma_{rz}^n(r)}{\mu} = A_1^n 2\frac{dr_2^n}{dr}\left[\gamma_1(r_n)(r_2^n)^{(\gamma_1(r_n)-1)} E_{\gamma_1(r_n)}(r_2^n) + (r_2^n)^{\gamma_1(r_n)} \frac{dE_{\gamma_1(r_n)}(r_2^n)}{d(r_2^n)}\right] + $$

$$A_2^n 2\frac{dr_2^n}{dr}\left[\gamma_1(r_n)(r_2^n)^{(\gamma_1(r_n)-1)} F_{\gamma_1(r_n)}(r_2^n) + (r_2^n)^{\gamma_1(r_n)} \frac{dF_{\gamma_1(r_n)}(r_2^n)}{d(r_2^n)}\right] + B_1^n\{-[\gamma(r_n)(\gamma(r_n)-$$

$$1)(\gamma(r_n) - 2)E_{\gamma(r_n)}(r_1^n) +$$

$$3\gamma(r_n)(\gamma(r_n) - 1)(r_1^n)^{(\gamma(r_n)-2)}\left(\frac{dr_1^n}{dr}\right)^3 \frac{dE_{\gamma(r_n)}(r_1^n)}{d(r_1^n)} +$$

$$3\gamma(r_n)(r_1^n)^{(\gamma(r_n)-1)}\left(\frac{dr_1^n}{dr}\right)^3 \frac{d^2E_{\gamma(r_n)}(r_1^n)}{d(r_1^n)^2} + (r_1^n)^{\gamma(r_n)}\left(\frac{dr_1^n}{dr}\right)^3 \times$$

$$\frac{d^3E_{\gamma(r_n)}(r_1^n)}{d(r_1^n)^3} - \frac{1}{(r_1^n)^2}\gamma(r_n)(r_1^n)^{(\gamma(r_n)-1)}\left(\frac{dr_1^n}{dr}\right)^3 E_{\gamma(r_n)}(r_1^n) -$$

$$\frac{1}{(r_1^n)^2}\gamma(r_n)(r_1^n)^{\gamma(r_n)}\left(\frac{dr_1^n}{dr}\right)^3 \frac{dE_{\gamma(r_n)}(r_1^n)}{d(r_1^n)} + \gamma(r_n)(\gamma(r_n) - 1) \times$$

$$\frac{1}{r_1^n}(r_1^n)^{(\gamma(r_n)-2)}\left(\frac{dr_1^n}{dr}\right)^3 E_{\gamma(r_n)}(r_1^n) + 2\gamma(r_n)\left(\frac{dr_1^n}{dr}\right)^3 \frac{1}{r_1^n}\frac{dE_{\gamma(r_n)}(r_1^n)}{d(r_1^n)} +$$

$$\frac{1}{r_1^n}(r_1^n)^{\gamma(r_n)}\left(\frac{dr_1^n}{dr}\right)^3 \frac{d^2E_{\gamma(r_n)}(r_1^n)}{d(r_1^n)^2}\Bigg] +$$

$$\frac{dr_1^n}{dr}\left[\boldsymbol{\gamma(r_n)(r_1^n)^{(\gamma(r_n)-1)}E_{\gamma(r_{n_i})}(r_1^n) + (r_1^n)^{(\gamma(r_n)-1)}\frac{dE_{\gamma(r_n)}(r_1^n)}{d(r_1^n)}}\right]\Bigg\} +$$

$$B_2^n\{-[\gamma(r_n)(\gamma(r_n) - 1)(\gamma(r_n) - 2) \times$$

$$F_{\gamma(r_n)}(r_1^n) + 3\gamma(r_n)(\gamma(r_n) - 1)(r_1^n)^{(\gamma(r_n)-2)}\left(\frac{dr_1^n}{dr}\right)^3 \frac{dF_{\gamma(r_n)}(r_1^n)}{d(r_1^{n_i})} +$$

$$\frac{d^3F_{\gamma(r_n)}(r_1^n)}{d(r_1^n)^3} - \frac{1}{(r_1^n)^2}\gamma(r_n)(r_1^n)^{(\gamma(r_n)-1)}\left(\frac{dr_1^n}{dr}\right)^3 F_{\gamma(r_n)}(r_1^n) -$$

$$\frac{1}{(r_1^n)^2}\gamma(r_n)(r_1^n)^{\gamma(r_n)}\left(\frac{dr_1^n}{dr}\right)^3 \frac{dF_{\gamma(r_n)}(r_1^n)}{d(r_1^n)} + \gamma(r_n)(\gamma(r_n) - 1) \times$$

$$\frac{1}{r_1^n}(r_1^n)^{(\gamma(r_n)-2)}\left(\frac{dr_1^n}{dr}\right)^3 F_{\gamma(r_n)}(r_1^n) + 2\gamma(r_n)\left(\frac{dr_1^n}{dr}\right)^3 \frac{1}{r_1^n} \times$$

$$\frac{dr_1^n}{dr}\left[\boldsymbol{\gamma(r_n)(r_1^n)^{(\gamma(r_n)-1)}F_{\gamma(r_n)}(r_1^n) + (r_1^n)^{(\gamma(r_n)-1)}\frac{dF_{\gamma(r_n)}(r_1^n)}{d(r_1^n)}}\right]\Bigg\}. \qquad (24)$$

This completes the consideration of the solution procedure to the system of Eqs. (2)-(5).

3.4 The solution to the field equations related to the fluid flow

According to (Guz 2009), we use the following representations for the solution to the system of Eqs. (6) and (7)

$$\rho' = -a_0^{-2}\rho_0 \frac{\partial}{\partial t}\Phi_f, \; p' = -\rho_0 \frac{\partial}{\partial t}\Phi_f, \; V_r = \frac{\partial}{\partial r}\Phi_f \,, \; V_z = \frac{\partial}{\partial z}\Phi_f, \qquad (25)$$

where the function Φ_f satisfies the equation

$$\left[\Delta - \frac{1}{a_0^2}\frac{\partial^2}{\partial t^2}\right]\Phi_f = 0 \,, \; \Delta = \frac{\partial^2}{\partial r^2} + \frac{1}{r}\frac{\partial}{\partial r} + \frac{\partial^2}{\partial z^2}. \qquad (26)$$

Representing the functions V_z, p' and ρ' by multiplying $\sin(kz - \omega t)$, and the functions Φ_f and V_r by multiplying $\cos(kz - \omega t)$, the following equation from (26) for Φ_{f1} (where $\Phi = \Phi_{f1}(r)\cos(kz - \omega t)$) is obtained.

$$\left(\frac{d^2}{dr_3^2} + \frac{1}{r_3}\frac{d}{dr_3} + 1\right)\Phi_{f1}(r) = 0 \,, \qquad (27)$$

where

$$r_3 = kr \sqrt{\left(\frac{c}{a_0}\right)^2 - 1} \, . \tag{28}$$

Taking the condition (11) into consideration, we find the solution to Eq. (27) as follows

$$\Phi_{f1}(r) = \begin{cases} FJ_0(r_3) \, if \, r_3^2 > 0 \\ FI_0(r_3) \, if \, r_3^2 < 0 \end{cases} \tag{29}$$

where $J_0(r_3)$ ($I_0(r_3)$) is the first kind of Bessel (modified Bessel) function of the zeroth order and F is an unknown constant.

Thus, substituting the function (29) through the relation $\Phi_f = \Phi_{f1}(r) \cos(kz - \omega t)$ into the expressions in (25), the following expressions for the quantities related to the fluid are obtained.

$$p' = \rho_0(V_z^0 k + \omega) \sin(kz - \omega t) \begin{cases} FJ_0(r_3) \, if \, r_3^2 > 0 \\ FI_0(r_3) \, if \, r_3^2 < 0 \end{cases},$$

$$\rho' = a_0^{-2} \rho_0(V_z^0 k + \omega) \sin(kz - \omega t) \begin{cases} FJ_0(r_3) \, if \, r_3^2 > 0 \\ FI_0(r_3) \, if \, r_3^2 < 0 \end{cases},$$

$$V_r = k \frac{dr_3}{dr} \cos(kz - \omega t) \begin{cases} -FJ_1(r_3) \, if \, r_3^2 > 0 \\ FI_1(r_3) \, if \, r_3^2 < 0 \end{cases}, V_z = -k \sin(kz - \omega t) \begin{cases} FJ_0(r_3) \, if \, r_3^2 > 0 \\ FI_0(r_3) \, if \, r_3^2 < 0 \end{cases} . \tag{30}$$

In this way, we determine the analytical expressions for all the quantities related to the hollow cylinder and fluid.

3.5 Obtaining the dispersion equation

By direct verification, it is determined that in the foregoing solution procedure $4N + 1$ number of unknown constants A_1^n, A_2^n, B_1^n, B_2^n ($n = 1,2,\ldots,N$) and F appear. As well as by direct verification, it is determined that the total number of the boundary, contact and compatibility conditions in (13) which contain these unknowns is also equal to $4N + 1$. Consequently, from the conditions in (13), we obtain the system of linear homogeneous equations with respect to these unknowns. According to the usual procedure, equating to zero the determinant of the coefficient matrix of these equations' system we obtain the following dispersion equation.

$$det(a_{nm}(c/c_2, kR, p_o/\mu, \frac{\rho}{\rho_0, h/R}, a_0/c_2)) = 0, n; m = 1,2,\ldots,4N + 1. \tag{31}$$

Here, we do not give the explicit expressions of the components a_{nm} of the coefficient matrix (a_{nm}) because these expressions can be easily determined from the expressions in (24) and (29). Note that the dispersion equation is solved numerically by employing the "bi-section" method. Now we consider the numerical results illustrating the influence of the inhomogeneous initial stresses in (1) on the dispersion of the axisymmetric longitudinal waves in the hydro-elastic system under consideration.

4. Numerical results and discussions

4.1 Testing the solution method and PC programs

First, we attempt to test the used solution method and for this purpose, we consider the case

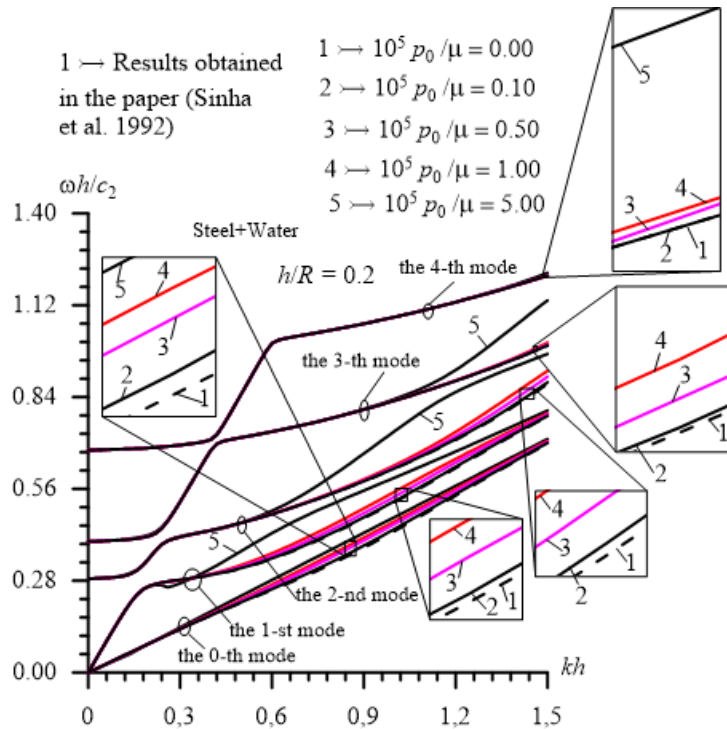*Surkay D. Akbarov and Gurbaneli J. Veliyev*

Fig. 2 Dispersion diagrams obtained for the zeroth and the first four modes and for various values of the ratio p_0/μ

which was also considered in the paper (Sinha *et al.* 1992), i.e., the case where the material of the cylinder is steel with the Lame constants $\lambda = 1.075 \times 10^{11}$ Pa and $\mu = 0.77 \times 10^{11}$ Pa, and with material density $\rho = 7910 \, \text{kg/m}^3$, and the fluid is water with sound speed velocity $a_0 = 1495 \, \text{m/sec}$ and density $\rho_0 = 1000 \, \text{kg/m}^3$. Moreover, as in the paper (Sinha *et al.* 1992), we assume that $h/R = 0.2$ and note that under obtaining all numerical results which will be considered below it is assumed that $N = 50$.

Thus, consider the numerical results which are obtained within the scope of the foregoing assumptions and which test the reliability of the used solution method, calculation algorithm and corresponding PC programs. These results are illustrated in Fig. 2 which show the dispersion diagrams, i.e., the graphs of the dependencies between $\omega h/c_2$, where $c_2 = \sqrt{\mu/\rho}$, and kh obtained for various values of the ratio p_0/μ which characterizes the magnitude of the inhomogeneous initial stresses.

The graphs are obtained for the so-called zeroth mode and for the first four modes. Note that in Fig. 2 the results related to the case where $p_0/\mu = 0$ which was also considered in the paper (Sinha *et al.* 1992) are drawn by dashed lines. Thus, comparison of the results obtained in the case where $p_0/\mu = 0$ and given in Fig. 2 with the corresponding ones given in the paper (Sinha *et al.* 1992) shows that they coincide completely with each other. Consequently, this gives a certain guarantee on the reliability of the proposed and used solution method and PC programs, according to which, the numerical results are obtained. Moreover, the results obtained in the case where $p_0/\mu > 0$ clearly show that under relatively great values of the dimensionless wavenumber kh, the
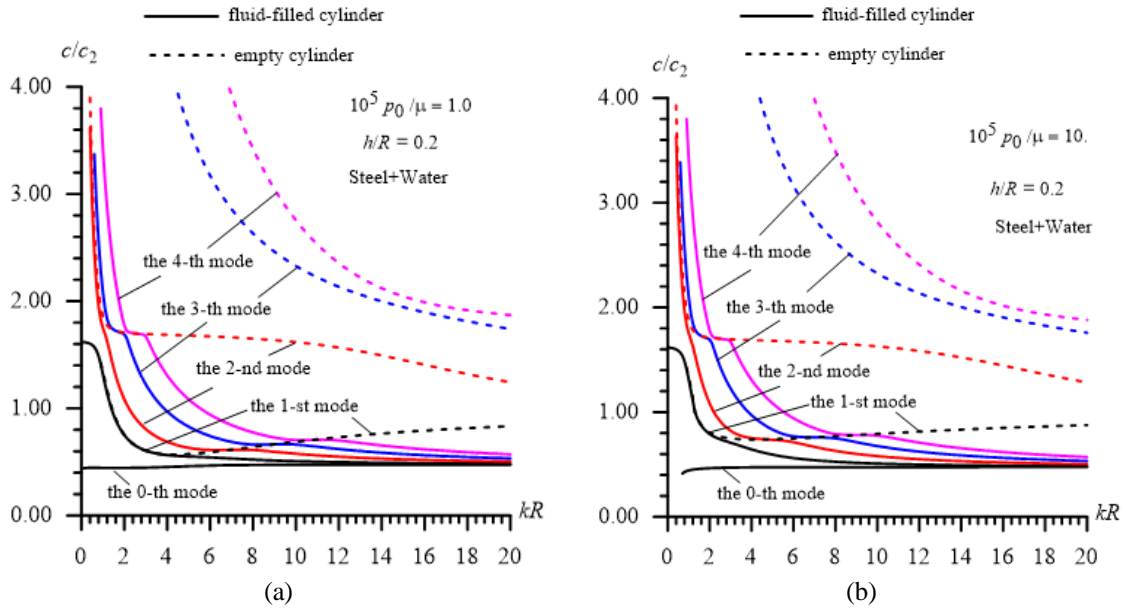
Fig. 3 Dispersion curves constructed in the cases where (a) $10^5 p_0/\mu = 1.0$ and (b) $10^5 p_0/\mu = 10.0$

internal fluid pressure on the inner surface of the cylinder causes to increase the wave propagation velocity in all the considered modes. Note that the zeroth mode is the mode with the slowest wave velocity and corresponds to the mode of the wave propagation in the "fluid cylinder".

We also consider the numerical results related to the dispersion curves obtained for the selected material properties for the cylinder and fluid. These curves are given in Fig. 3 which are obtained in the cases where $10^5 p_0/\mu = 1.0$ (Fig. 3(a)) and $10^5 p_0/\mu = 10.0$ (Fig. 3(b)). At the same time, in Fig. 3 the dispersion curves obtained for the empty cylinder are also given and these curves are drawn by the dashed lines. According to Fig. 3, it can be concluded that the existence of the fluid causes to decrease significantly the wave propagation velocity in the first, second, third and fourth modes. Moreover, it follows from Fig. 3 that the zeroth mode appears as a result of the existence of the fluid in the cylinder and this mode is sometimes called "quasi-Scholte" waves, and the wave propagation velocity in this mode approaches the wave propagation velocity of the corresponding Scholte wave as $kR \to \infty$. We recall that the Schott wave is the near-surface non-dispersive wave (similar to the Stoneley wave) which appears near the interface plane between the semi-infinite fluid and semi-infinite elastic medium. The results illustrated in Fig. 3 also confirm in the qualitative sense the reliability of the solution method and calculation algorithm used in the present investigation.

Finally, we illustrate the numerical results in terms of their convergence with respect to the number N and, for this purpose, we consider the graphs in Fig. 4, which show the dispersion curves obtained for the pair steel+Glycerin in the zeroth (Fig. 4(a)) and first (Fig. 4(b)) modes and for the pair steel+water in the first mode (Fig. 4(c)). In the construction of the dispersion curves for the steel+Glycerin pair, the speed of sound and the density for the Glycerin are assumed to be $a_0 = 1927$ m/sec and $\rho_0 = 1260$ kg/m^3, respectively. As can be seen from Fig. 4, increasing the values of the number N affects the character of the considered dispersion curves not only in a quantitative but also in a qualitative sense. However, above a certain value of the number N, the
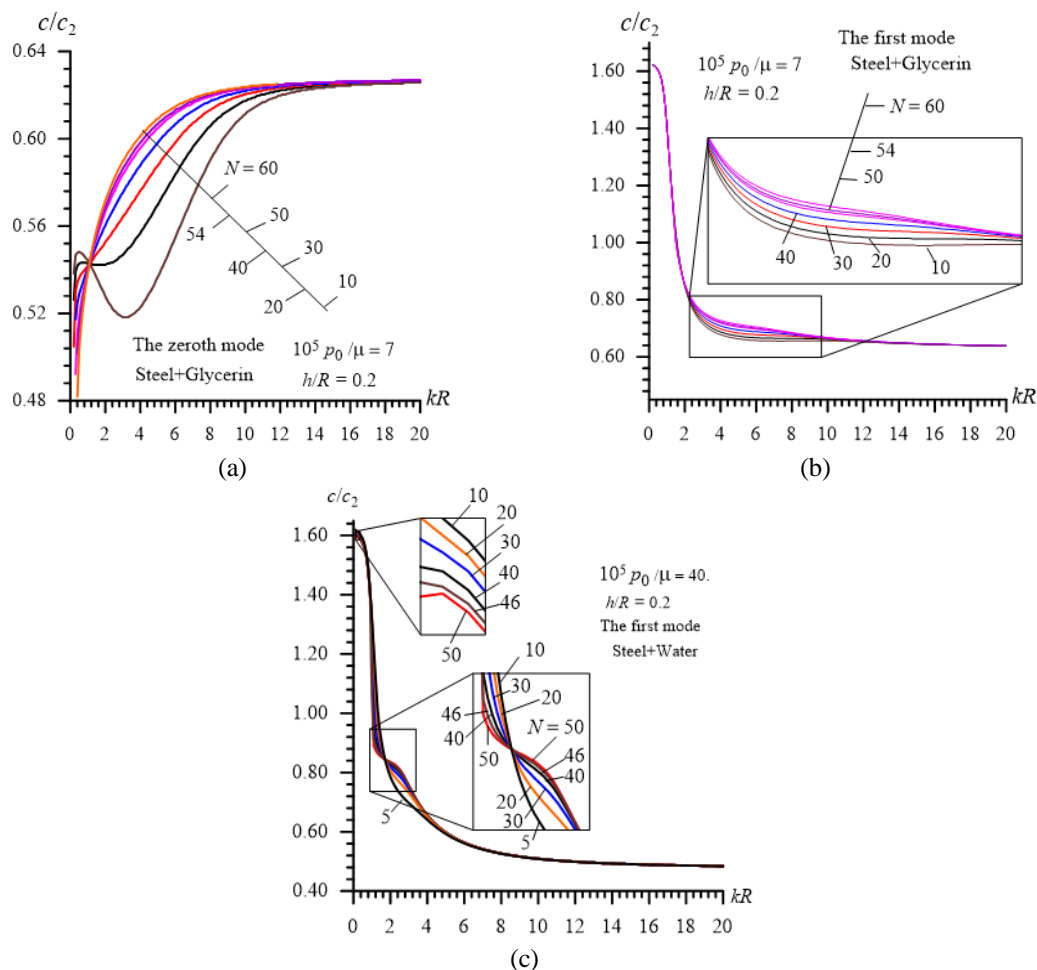
Fig. 4 Convergence of the numerical results with respect to the number N for the steel+glycerin in the zeroth (a), and first (b) modes and for the steel+water pair (c) in the first mode

influence of the further increase of the value of this number on the dispersion curves becomes insignificant. Note that these results and other related results show that the number $N = 50$ is quite sufficient to obtain results with high accuracy. In determining this number, the criterion $\int_{0.01}^{20}((c/c_2)_N - (c/c_2)_{N-1})d(kR) \leq 10^{-4}$ is used. Note that when considering the higher modes, the convergence of the numerical results leaves no doubt. This is because after is $N \geq 20$, the results obtained for each N agree with an accuracy of less than 10^{-4}. Moreover, no instability of the calculations was observed in the numerical results presented in this paper.

This completes the testing of the solution method, calculation algorithm and PC programs applied under obtaining numerical results which will be considered and analyzed below.

4.2 Parametric study of the influence of the initial stresses on the wave dispersion

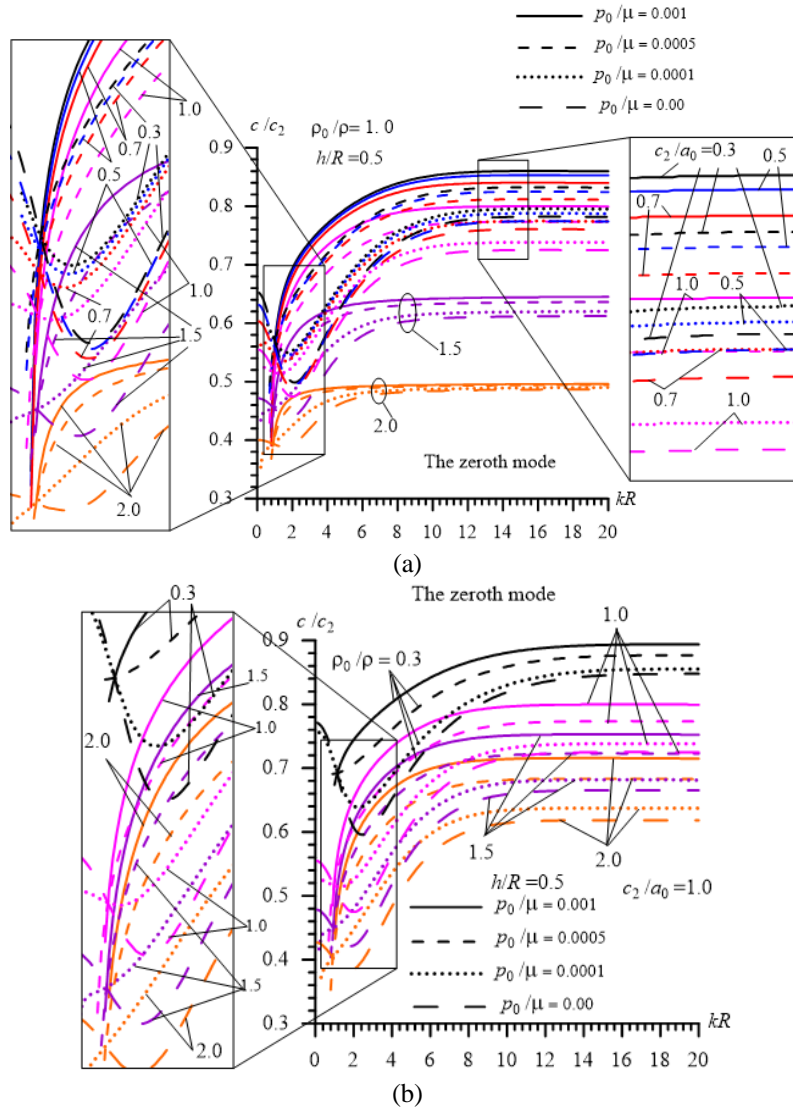We introduce the dimensionless parameters c_2/a_0, ρ_0/ρ and h/R (where c_2 is the shear wave

Fig. 5 The influence of the rations c_2/a_0 (a) and ρ_0/ρ (b) on the dispersion curves of the zeroth mode

propagation in the cylinder material, a_0 is the sound speed in the fluid, ρ is the density of the cylinder material, ρ_0 is the density of the fluid, h is the cylinder thickness, and R is the inner radius of the cylinder's cross section) and investigate their effect on the influence of the values of the ratio p_0/μ which characterize the magnitude of the inhomogeneous initial stresses in the cylinder (where p_0 is the fluid pressure in the initial state and μ is the shear modulus of the plate material) on the dispersion curves, i.e., the graphs of the dependence between c/c_2 and kR.

It should be noted that the change of the selected dimensionless parameters influences not only the dynamic behavior of the hydro-elastic systems but also the convergence of the numerical methods used for the solution of these problems (see, for instance, the paper (Ha and Choi 2020)).

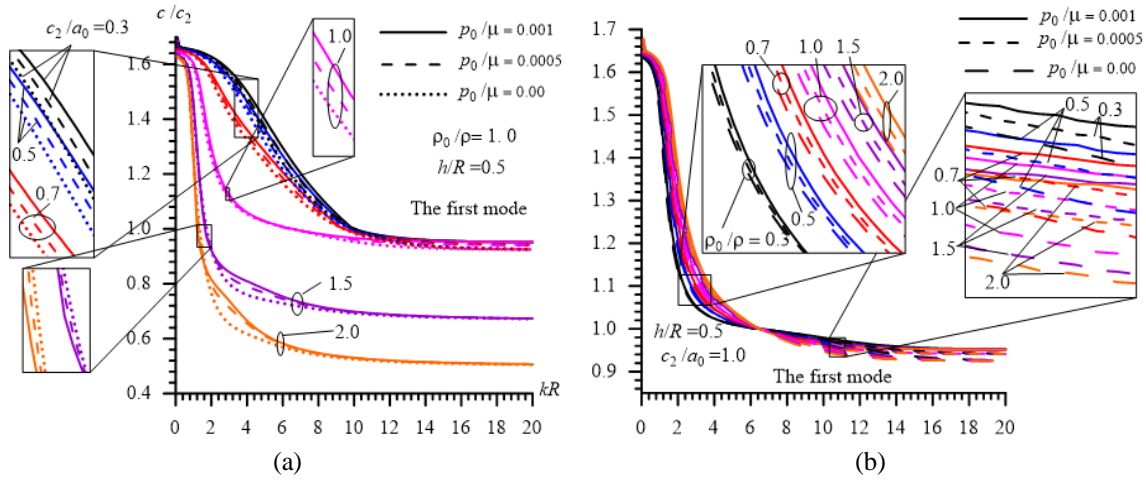Thus, we make this investigation for the zeroth, first, second and third modes and first, we

Fig. 6 The influence of the rations c_2/a_0 (a) and ρ_0/ρ (b) on the dispersion curves of the first mode
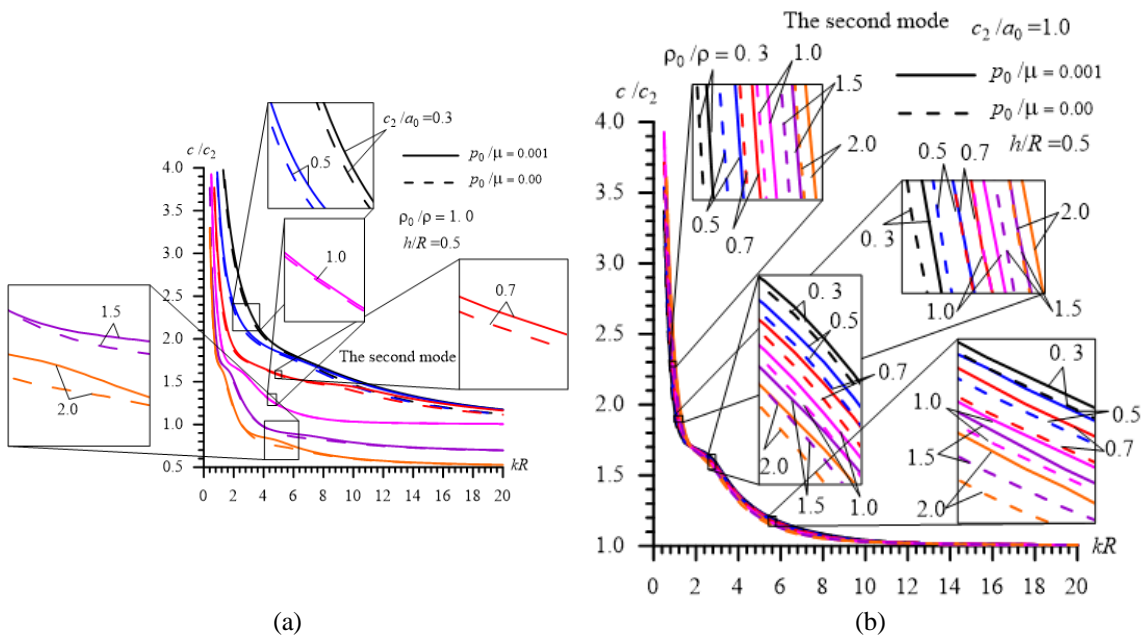

Fig. 7 The influence of the rations c_2/a_0 (a) and ρ_0/ρ (b) on the dispersion curves of the second mode

analyze the numerical results illustrating the character of the influence of the ratios c_2/a_0 (under fixed ρ_0/ρ) and ρ_0/ρ (under fixed c_2/a_0) on the dispersion curves under the fixed value of h/R which for the cases under consideration is selected as $h/R = 0.5$ (unless otherwise specified). For this purpose, consider the dispersion curves given in Figs. 5, 6, 7 and 8 which are related to the zeroth, first, second and third modes, respectively. In these figures, the graphs grouped by the letters *a* and *b* show the influence of the change of the ratios c_2/a_0 and ρ_0/ρ respectively on the dispersion curves.

Thus, it follows from these results that in all the considered modes an increase in the values of
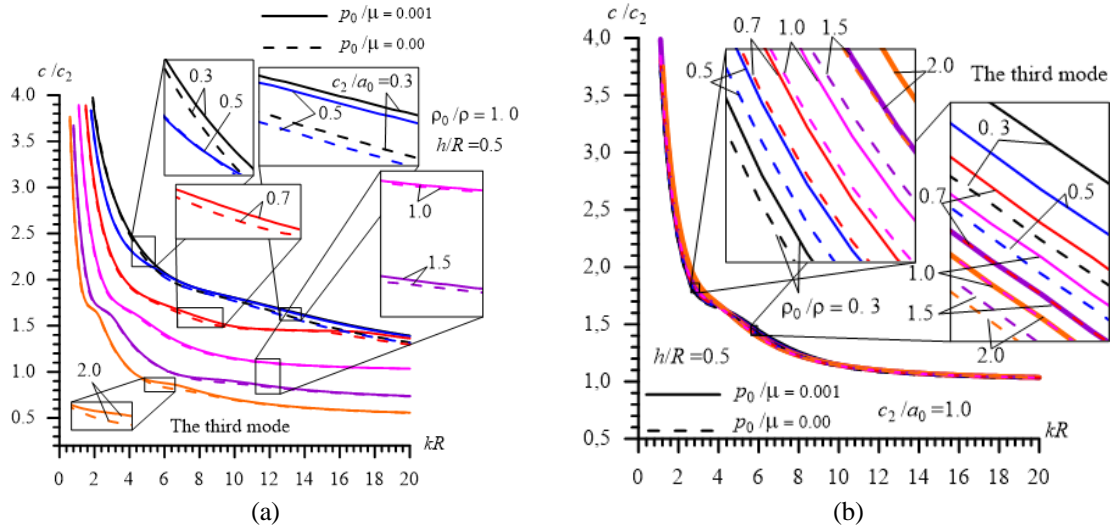
Fig. 8 The influence of the ratios (a) c_2/a_0 and (b) ρ_0/ρ on the dispersion curves of the third mode
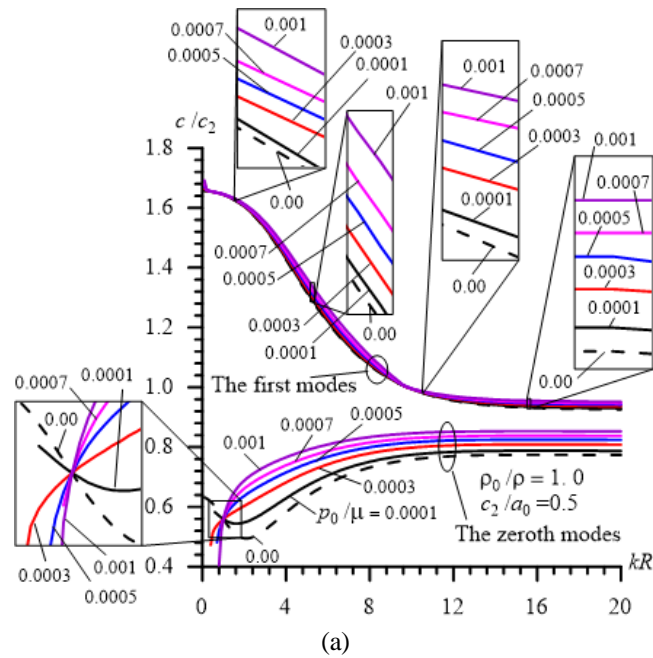

Fig. 9 The influence of the magnitude of the inhomogeneous initial stresses on the dispersion curves obtained under $h/R = 0.5$

the ratio c_2/a_0 causes a decrease in the values of the wave propagation velocity. Moreover, in the zeroth mode, an increase in the values of the ratio ρ_0/ρ also causes a decrease in the velocity of the wave propagation velocity. However, in the first, second and third modes, the character of the influence of the ratio ρ_0/ρ on the wave propagation velocity depends on the dimensionless wavenumber. In other words, there exists such a value of kR (denote it by $(kR)'$) before which,
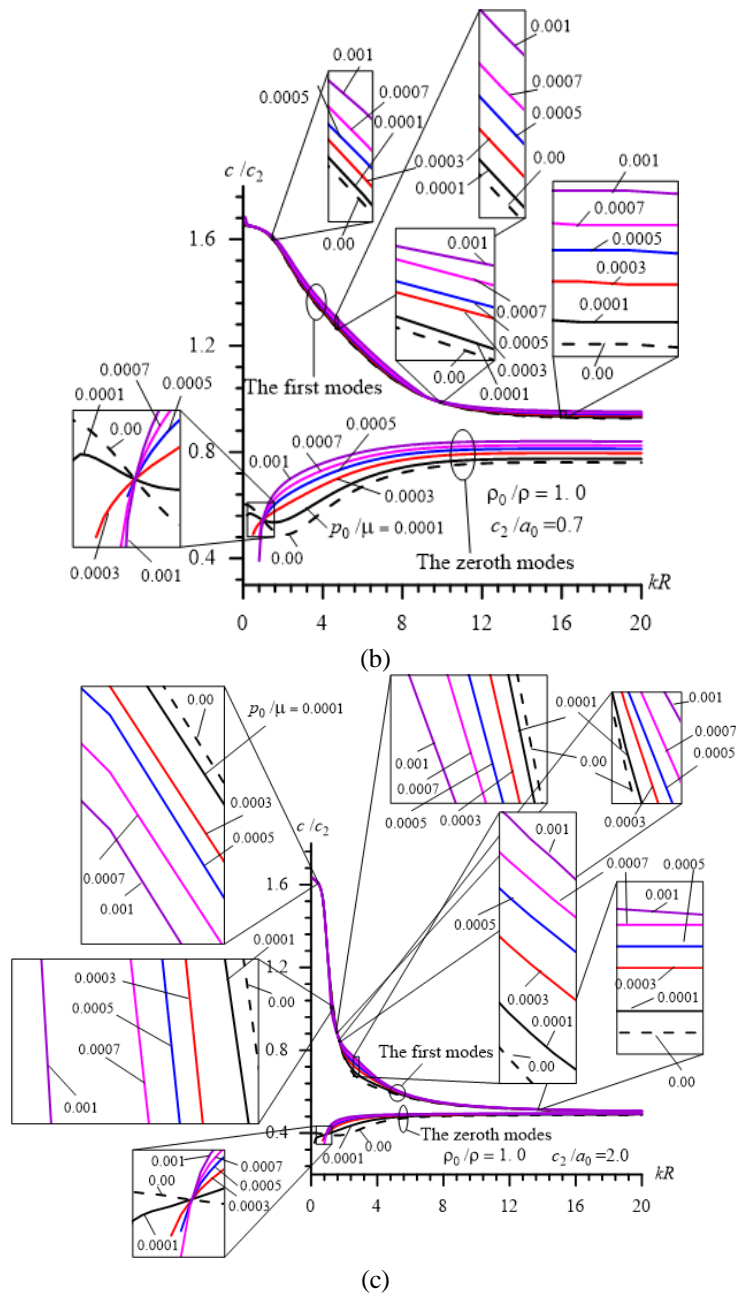
(b)

(c)

Fig. 9 Continued

i.e., under $kR < (kR)'$, the increase in the values of the ratio ρ_0/ρ causes an increase in the wave propagation velocity, however, after that value, i.e., under $kR > (kR)'$ the increase in the values of the ratio ρ_0/ρ causes a decrease in the wave propagation velocity.

    The results also show that in the quantitative sense the magnitude of the influence of the ratio c_2/a_0 on the wave propagation velocity is more considerable than that of the ratio ρ_0/ρ At the

same time, these results show that in all the cases under consideration an increase in the values of the ratio p_0/μ, i.e., an increase in the values of the pressure acting on the interior of the cylinder causes an increase in the magnitude of the influence of the initial stresses on the values of the wave propagation velocity.

Now we consider in more detail numerical results illustrating how this internal pressure, i.e., the magnitude of the inhomogeneous initial stresses influences the dispersion curves in the qualitative and quantitative sense. For this purpose, we consider the case where $\rho_0/\rho = 1.0$ and analyze the graphs given in Fig. 9 which are obtained in the cases where $c_2/a_0 = 0.5$ (Fig. 9(a)), 0.7 (Fig. 9(b)) and 2.0 (Fig. 9(c)) under various values of the ratio p_0/μ for the zeroth and first modes. It follows from these results that the dispersion curves related to the zeroth mode not only in the quantitative sense but also in the qualitative sense depend significantly on the values of p_0/μ. As follows from these results, in the zeroth mode in the case where $p_0/\mu = 0$ the dependence between c/c_2 and kR has non-monotonic character. However, by increasing the values of p_0/μ the dependence becomes monotonic. Moreover, these results show that the character of the influence of p_0/μ on the values of the wave propagation velocity in the zeroth mode depends on the dimensionless wavenumber kR. There exists such a value of kR (denote it by $(kR)^*$) before which, i.e., in the cases where $kR < (kR)*$ an increase in the values of p_0/μ causes a decrease in the wave propagation velocity in the zeroth mode, however, after which, i.e., in the cases where $kR > (kR)*$ an increase in the values of p_0/μ causes an increase in the wave propagation velocity in the zeroth mode. At the same time, the magnitude of these "decreases" and "increases" grows monotonically with p_0/μ. Besides all of these, the results show that as a result of the existence of inhomogeneous initial stresses in the cylinder, the cut off wavelength appears for the dispersion curves of the zeroth mode and the values of these wavelengths increase with p_0/μ.

Analyses of the dispersion curves related to the first mode show that in the relatively small values of c_2/a_0, i.e., in the cases where $c_2/a_0 = 0.5$ and 0.7, the wave propagation velocity increases with p_0/μ for all the values of kR. However, the magnitude of this increase depends significantly on kR, and there exists such a value of kR (denote it by $(kR)_1$)) for $kR < (kR)_1$ where the influence of the initial stresses on the wave propagation velocity increase with kR, however, for $kR > (kR)_1$ this influence decreases monotonically with kR, and this decreasing continues before a certain value of kR (denote it by $(kR)_2$), and under $kR = (kR)_2$ the magnitude of the influence becomes the minimum. At the same time, for the cases where $kR > (kR)_2$, the influence starts to increase again with kR.

For instance, under $c_2/a_0 = 0.5$ in the cases where $kR < 5$ (i.e., $(kR)_1 = 5$) the magnitude of the influence increases monotonically with kR, however, under $5 < kR < 10$ (i.e., $(kR)_2 = 10$) this magnitude decreases monotonically with kR. Finally, after $kR = 10$, i.e., in the cases where $kR > 10$, the magnitude of the "increase" grows with kR. Note that similar results are also obtained for the cases where $c_2/a_0 = 0.7$. However, under relatively great values of c_2/a_0, for instance in the case where $c_2/a_0 = 2.0$ (Fig. 8(c)) in the low wavenumber approximation, the existence of the inhomogeneous initial stresses causes to decrease the wave propagation velocity and the magnitude of this "decrease" increases with p_0/μ. Note that this conclusion in the qualitative sense agrees with the corresponding results obtained in the paper (Atabek and Lew 1966) in which steel is taken as the cylinder material and water is taken as the fluid for which $c_2/a_0 \approx 2.11$. However, in the paper (Atabek and Lew 1966), the numerical results related to the higher wavenumber approximation are not given. Thus, it follows from Fig. 9(c) that in the high wavenumber approximation, the existence of the inhomogeneous initial stresses in the cylinder
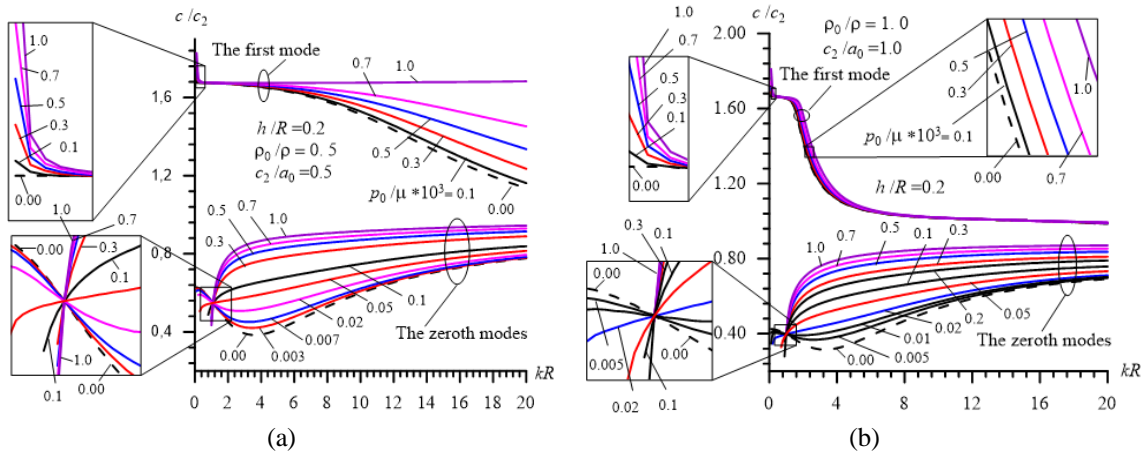
Fig. 10 Dispersion curves obtained for the case where $h/R = 0.2$ under (a) c_2/a_0=0.5, $\rho_0/\rho = 0.5$ and (b) c_2/a_0=1.0, $\rho_0/\rho = 1.0$
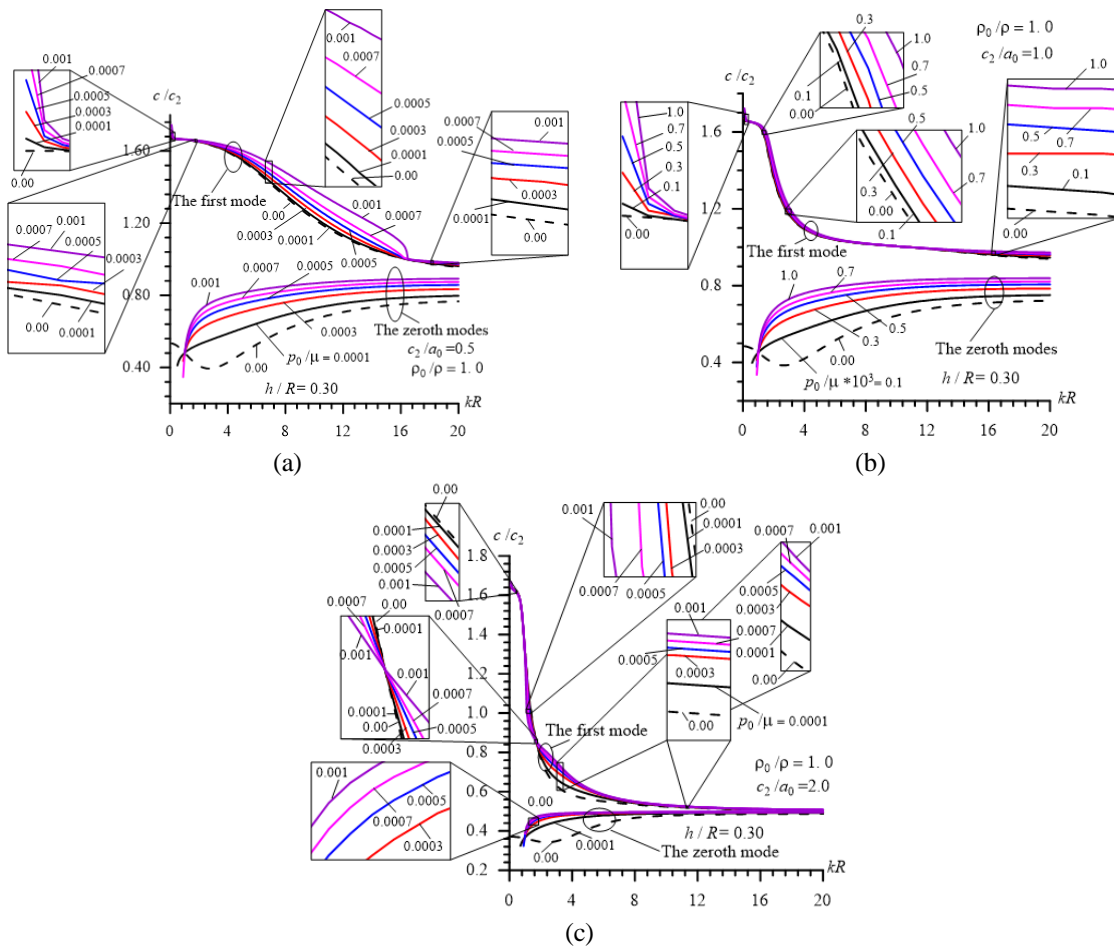

Fig. 11 Dispersion curves obtained for the case where $h/R = 0.3$ and $\rho_0/\rho = 1.0$ under (a) c_2/a_0= 0.5, (b) c_2/a_0=1.0 and (c) c_2/a_0=2.0
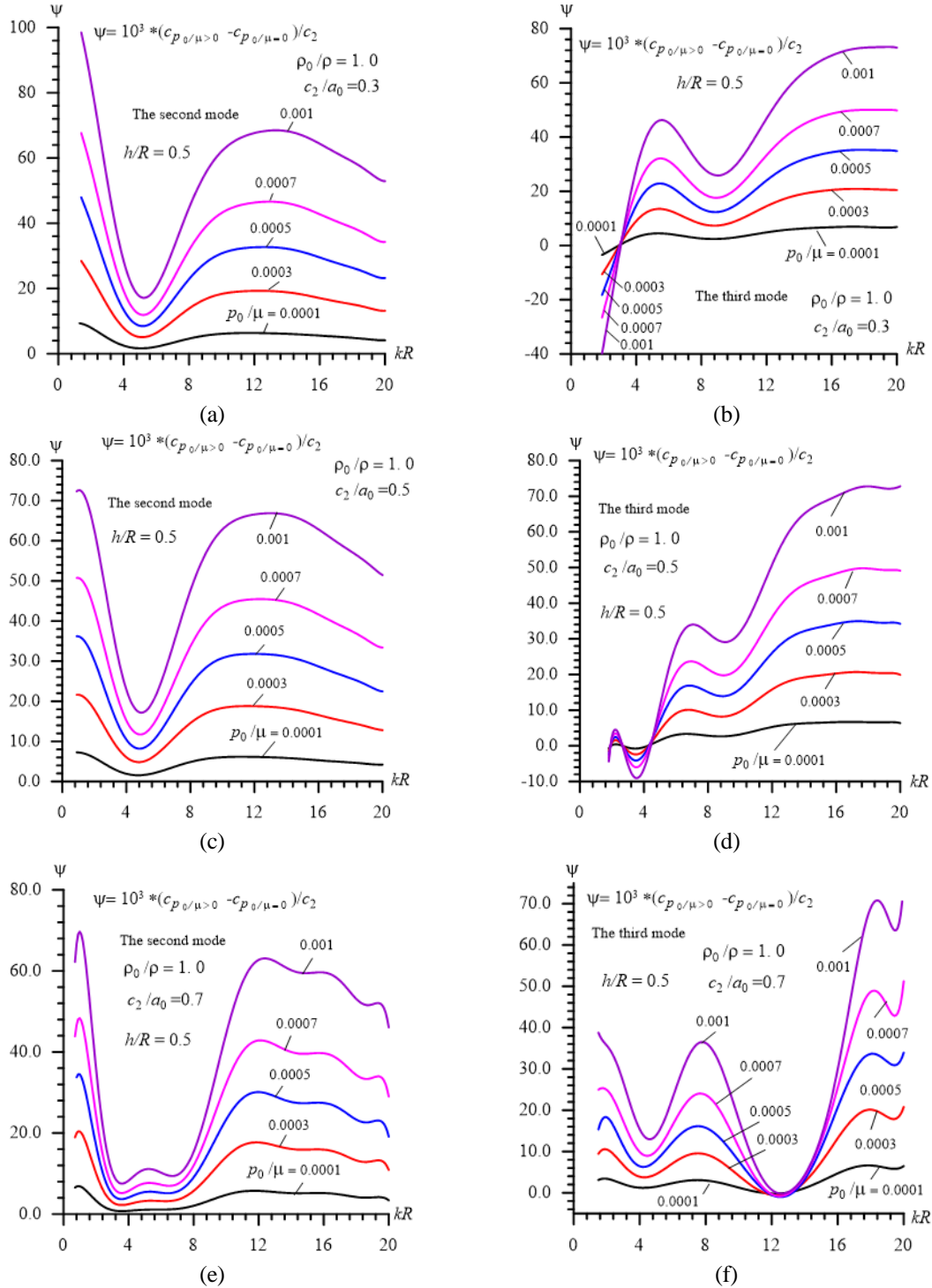
Fig. 12 The influence of the inhomogeneous initial stresses on the wave propagation velocity in the second and third modes
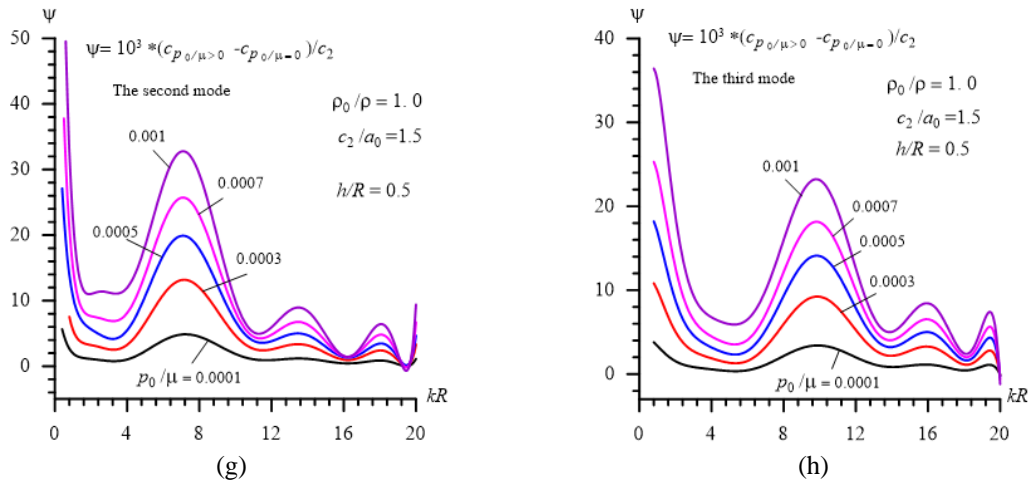
(g)   (h)

Fig. 12 Continued

causes the wave propagation velocity to increase in the first mode and the magnitude of this "increase" grows monotonically with p_0/μ. Here, we do not consider the corresponding results obtained for various ρ_0/ρ because the effect of the change ρ_0/ρ does not have as much effect as the change c_2/a_0.

Note that the foregoing results are obtained for the case where $h/R = 0.5$, and for investigation of how the change of the ratio h/R influences the dispersion curves, we consider the graphs given in Figs. 10 and 11 which are constructed in the cases where $h/R = 0.2$ and 0.3, respectively.

It follows from these results that under relatively small values of the ratio h/R and under relatively small values of the ratio c_2/a_0 (Fig. 10(a) and Fig. 11(a)), the influence of the initial inhomogeneous stresses on the dispersion curves becomes more considerable, not only for the zeroth approximation but also for the first approximation. According to the foregoing discussions, it can be concluded that under relatively small values of the ratio c_2/a_0, the values of $(kR)_1$ and $(kR)_2$, which are indicated above, increase with decreasing of h/R. For instance, it follows from Fig. 10(a) that $(kR)_1 > 20$ in the case where $h/R = 0.2$, and it follows from Fig. 11(a) that $(kR)_1 > 12$. At the same time, the results shown in Figs. 10(b), 11(b) and 11(c) illustrate that an increase in the values of the ratio c_2/a_0 causes a decrease in the magnitude of the influence of the inhomogeneous initial stresses on the wave propagation velocity in the first mode for all the considered values of h/R.

Besides all of these, the results given in Figs. 10 and 11 show that the inhomogeneous initial stresses in the cylinder cause the cut off wavelength to appear not only in the zeroth mode but also causes the cut off frequency to appear in the first mode and this appearance is more clearly observed in the relatively small values of the ratio h/R and the values of these cut off frequencies increase with p_0/μ.

At the same time, it follows from Fig. 11(c) that under relatively great values of the ratio c_2/a_0 the character of the influence of the inhomogeneous initial stresses on the wave propagation velocity in the first mode depends on the values of kR. This is because, in the low wavenumber approximation the initial stresses cause to decrease the wave propagation velocity in the first mode, however, in the moderate and high wavenumber approximations they cause to increase the

wave propagation velocity in the first mode. We recall that such results were also obtained for the Steel+Water system which is discussed above and these results agree in the qualitative sense with the corresponding results obtained in the paper (Atabek and Lew 1966).

Finally, we consider the results which show the influence of the initial inhomogeneous initial stresses on the wave propagation velocity in the second and third modes. These results are given in Fig. 12 which are obtained in the cases where $c_2/a_0 = 0.3$ (Fig. 12(a) and (b)), 0.5 (Fig. 12(c) and (d)), 0.7 (Fig. 12(e) and (f)) and 1.5 (Fig. 12(f) and (g)) under $\rho_0/\rho = 1.0$ and $h/R = 0.5$. In this figure the graphs grouped by letters a, c, e and g ((b), (d), (f) and (h)) relate to the second (to the third) mode.

In the second and third modes the magnitude of the influence of the initial inhomogeneous stresses on the wave propagation velocity is not as much as in the zeroth and first approximation, therefore, for a clear illustration of the results in Fig. 12 the following parameter is used

$$\psi = 10^3 (c|_{p_0/\mu>0} - c|_{p_0/\mu=0})/c_2 \qquad (32)$$

and through this parameter the specified influence is estimated.

Thus, it follows from Fig. 12 that in all cases, the initial stresses cause to increase the wave propagation velocity in the second mode, however, in the third mode the character of the influence of the initial stresses on the wave propagation velocity depends on the values of the ratio c_2/a_0 and h/R. For instance, in the cases where $c_2/a_0 = 0.3$ and 0.5 under relatively small values of kR, the initial stresses cause to decrease the wave propagation velocity, however, under relatively great values the initial stresses cause to increase the wave propagation velocity. At the same time, in the cases where $c_2/a_0 = 0.7$ and 1.5, for almost all the considered values of kR, the initial stresses cause to increase the wave propagation velocity.

This completes the analyzes of the numerical results related to the parametric study of the influence of the inhomogeneous initial stresses in the hollow cylinder containing the compressible inviscid fluid on the dispersion of the axisymmetric waves propagating in this cylinder.

5. Conclusions

In the present work, the dispersion of axisymmetric longitudinal waves propagating in a hydro elastic system consisting of a hollow cylinder with inhomogeneous initial stresses and a non-viscous compressible fluid in this cylinder has been studied. In the context of this study, the motion of the cylinder is described in the framework of the so-called three-dimensional linearized theory of elastic waves in bodies with initial stresses and the flow of the inviscid compressible fluid is described in the framework of the linearized Euler equations. It is assumed that the initial static inhomogeneous stresses in the cylinder occur as a consequence of the fluid pressure and that these stresses are determined by using the corresponding known expressions. The solution of the wave equations related to the cylinder is solved by using the discrete analytical solution method and the corresponding dispersion equation is obtained. The algorithm and the programs PC have been developed for the numerical solution of the dispersion equation and both this algorithm and the programs have been tested for the case when the material of the cylinder is steel and the fluid is water. In this particular case, the presented numerical results are compared with the corresponding results of other authors and in this way the reliability, accuracy and convergence of the used algorithm and programs are proved.

We introduced the dimensionless parameters c_2/a_0, ρ_0/ρ and h/R (where c_2 is the shear wave

propagation in the cylinder material, a_0 is the sound speed in the fluid, ρ is the density of the cylinder material, ρ_0 is the density of the fluid, h is the cylinder thickness, and R is the inner radius of the cylinder's cross section) and we investigated their effect on the influence of the values of the ratio p_0/μ which characterizes the magnitude of the inhomogeneous initial stresses in the cylinder (where p_0 is the fluid pressure in the initial state and μ is the shear modulus of the plate material) on the dispersion curves, i.e., the graphs of the dependence between c/c_2 and kR. This influence is investigated for the zeroth, first, second and third modes.

Numerical results are presented on the indicated influence and the following corresponding concrete conclusions are made. Here we attempt to formulate some of them:

- The influence of the ratio c_2/a_0 on the dispersion curves and on the magnitude of the effect of the initial stresses on the dispersion curves is more considerable than that of the ratio ρ_0/ρ;
- An increase in the values of the ratios c_2/a_0 and ρ_0/ρ causes to decrease the wave propagation velocity and the magnitude of the influence of the inhomogeneous initial stresses on the wave propagation velocity;
- A decrease in the values of the ratio h/R causes to increase the magnitude of the influence of the inhomogeneous initial stresses on the wave propagation velocity and this magnitude increases monotonically with p_0/μ;
- The influence of the inhomogeneous initial stresses on the dispersion curves related to the zeroth mode changes these curves not only in the quantitative sense but also in the qualitative sense. There exists such a value of the dimensionless wavenumber kR (denoted by $(kR)*$) before which, i.e., under $kR < (kR)*$ an increase in the values of the ratio p_0/μ causes to decrease the wave propagation velocity in the zeroth mode, however, after which, i.e., under $kR > (kR)*$ it causes to increase the wave propagation velocity in the zeroth mode and the value of $(kR)*$ does not depend on p_0/μ;
- The character of the influence of the inhomogeneous initial stresses on the wave propagation in the first mode depends not only on the ratio c_2/a_0 and the dimensionless wavenumber kR, but also on the ratio h/R;
- The influence of the inhomogeneous initial stresses in the cylinder on the wave propagation velocity in the zeroth and first modes is more considerable than in the second and third modes;
- In the relatively great values of the ratio c_2/a_0 under low wavenumber approximation, initial inhomogeneous initial stresses cause the wave propagation velocity in the first mode to decrease. However, under moderate and high wavenumber approximations they cause the wave propagation velocity in the first mode to increase;
- As a result of the existence of the inhomogeneous initial stresses, the cut off wavelength in the zeroth approximation and the cut off frequencies in the first mode appear.

At the same time, in the body of the paper many other concrete conclusions are made related to the dynamics of the hydro-elastic system under consideration.

References

Ahmed, S.S. (2008), "Axially symmetric vibrations of fluid-filled poroelastic circular cylindrical shells", *J. Sound Vib.*, **318**, 389-405. https://doi.org/10.1016/j.jsv.2008.04.012.

Akbarov, S.D. (2015), *Dynamics of Pre-Strained Bi-Material Elastic Systems: Linearized Three-Dimensional Approach*, Springer, Heidelberg, New York, USA.

Akbarov, S.D. (2018), "Forced vibration of the hydro-viscoelastic and -elastic systems consisting of the

viscoelastic or elastic plate, compressible viscous fluid and rigid wall: A review", *Appl. Comput. Math.*, **17**, 221-245.

Akbarov, S.D. and Bagirov, E.T. (2019), "Axisymmetric longitudinal wave dispersion in a bi-layered circular cylinder with inhomogeneous initial stresses", *J. Sound Vib.*, **450**, 1-27. https://doi.org/10.1016/j.jsv.2019.03.003.

Akbarov, S.D. and Huseynova, T.V. (2019), "Forced vibration of the hydro-elastic system consisting of the orthotropic plate, compressible viscous fluid and rigid wall", *Couple. Syst. Mech.*, **8**, 199-218. https://doi.org/10.12989/csm.2019.8.3.199.

Akbarov, S.D. and Huseynova, T.V. (2020), "Fluid flow profile in the "orthotropic plate+compressible viscous fluid+rigid wall" system under the action of the moving load on the plate", *Couple. Syst. Mech.*, **9**, 289-309. https://doi.org/10.12989/csm.2020.9.3.289.

Akbarov, S.D., Sevdimaliyev, Y.M. and Valiyev, G.J. (2021), "Mathematical modeling of the dynamics of a hydroelastic system-A hollow cylinder with inhomogeneous initial stresses and compressible fluid", *Math. Meth. Appl. Sci.*, **44**(9), 7858-7872. https://doi.org/10.1002/mma.7329.

Atabek, H.B. (1968), "Wave propagation through a viscous fluid contained in a tethered initially stressed, orthotropic elastic tube", *Biophys. J.*, **8**, 626-649.

Atabek, H.B. and Lew, H.S. (1966), "Wave propagation through a viscous incompressible fluid contained in an initially stressed elastic tube", *Biophys. J.*, **6**, 481-503.

Bagno, A.M. and Guz, A.N. (1982), "Wave propagation in a previously stressed, incompressible cylinder containing a viscous compressible liquid", *Mech. Compos. Mater.*, **2**, 349-355. https://doi.org/10.1007/BF00604851.

Bagno, A.M. and Guz, A.N. (1997), "Elastic waves in prestressed bodies interacting with fluid (Survey)", *Int. Appl. Mech.*, **33**, 435-465. https://doi.org/10.1007/BF02700652.

Bagno, A.M. and Guz, A.N. (2016), "Effect of prestresses on the dispersion of waves in a system consisting of a viscous liquid layer and a compressible elastic layer", *Int. Appl. Mech.*, **52**, 333-341. https://doi.org/10.1007/s10778-016-0756-4.

Bagno, A.M., Guz, A.N. and Efremov, V.I. (1994), "Effect of initial strains on the propagation of waves in an incompressible cylinder located in an ideal fluid", *Int. Appl. Mech.*, **30**, 583-585. https://doi.org/10.1007/BF00847229.

Bochkarev, S.A. and Lekomtsev, S. V. (2022), "Natural vibrations and hydroelastic stability of laminated composite circular cylindrical shells", *Struct. Eng. Mech.*, **81**(6), 769-780. https://doi.org/10.12989/sem.2022.81.6.769.

Darıcık, F., Canbolat, G. and Koru, M. (2022), "Investigation of a fiber reinforced polymer composite tube by two way coupling fluid-structure interaction", *Couple. Syst. Mech.*, **11**(4), 315-333. https://doi.org/10.12989/csm.2022.11.4.315.

Eringen, A.C. and Suhubi, E.S. (1975), *Elastodynamics*, *Finite Motion*, *Vol. I; Linear Theory*, *Vol. II*, Academic Press, New York.

Gao, H., Li, X., Nezhad, A.H. and Behshad, A. (2022), "Numerical simulation of the flow in pipes with numerical models", *Struct. Eng. Mech.*, **81**(4), 523-527. https://doi.org/10.12989/sem.2022.81.4.523.

Guz, A.N. (2004), *Elastic Waves in Bodies with Initial (Residual) Stresses*, A.C.K. Kiev. (in Russian)

Guz, A.N. (2009), *Dynamics of Compressible Viscous Fluid*, Cambridge Scientific Publishers.

Ha, S.T. and Choi, H.G. (2020), "Investigation on the effect of density ratio on the convergence behavior of partitioned method for fluid-structure interaction simulation", *J. Fluid. Struct.*, **96**, 103050. https://doi.org/10.1016/j.jfluidstructs.2020.103050.

Hadzalic, E., Ibrahimbegovic, A. and Dolarevic, S. (2018), "Fluid-structure interaction system predicting both internal pore pressure and outside hydrodynamic pressure", *Couple. Syst. Mech.*, **7**(6), 649-668. https://doi.org/10.12989/csm.2018.7.6.649.

Kumar, G.M. and Sriram, V. (2020), "Development of a hybrid model based on mesh and meshfree methods and its application to fluid-elastic structure interaction for free surface waves", *J. Fluid. Struct.*, **99**, 103159. https://doi.org/10.1016/j.jfluidstructs.2020.103159.

Lamb, H. (1898), "On the velocity of sound in a tube, as affected by the elasticity of the walls", *Manchester*

Memoirs, **42**, 1-16.

Lin, T.C. and Morgan, G.W. (1956), "Wave propagation through fluid contained in a cylindrical, elastic shell", *J. Acoust. Soc. Am.*, **28**, 1165-1176.

Mandal, K.K. and Maity, D. (2015), "2d finite element analysis of rectangular water tank with separator wall using direct coupling", *Couple. Syst. Mech.*, **4**(4), 317-336. https://doi.org/10.12989/csm.2013.2.2.127.

Plona, T.J., Sinha, B.K., Kostek, S. and Chong, S.K. (1992), "Axisymmetric wave propagation in fluid loaded cylindrical shells. II. Theory versus experiment", *J. Acoust. Soc. Am.*, **92**, 1144-1155. https://doi.org/10.1121/1.404041.

Rachev, A.I. (1978), "Propagation of a pulse wave in arteries taking account of prior stresses and muscle activity", *Mekh. Polim.*, **2**, 244-252.

Sandhyarani, B., Rao, J.A. and Reddy, P.M. (2019), "Axially symmetric vibrations of a liquid-filled poroelastic thin cylinder saturated with two immiscible liquids surrounded by a liquid", *J. Fluid. Struct.*, **11**, 272-280. https://doi.org/10.22034/JSM.2019.665907.

Selvamani, R. (2016), "Dispersion analysis in a fluid-filled and immersed transversely isotropic thermos-electro-elastic hollow cylinder", *Mech. Mech. Eng.*, **20**, 209-231.

Sinha, B.K., Plona, T.J., Kostek, S. and Chong, S.-K. (1992), "Axisymmetric wave propagation in fluid loaded cylindrical shells. I: Theory", *J. Acoust. Soc. Am.*, **92**(2), 1132-1143. https://doi.org/10.1121/1.404040.

Timoshenko S. and Goodier, J.N. (1951). *Theory of elasticity*, McGraw-Hill.

Watson, G.N. (1966), *A Treatise on the Theory of Bessel Functions*, 2nd Edition, Cambridge University Press.

CC